PD IEC/TR 62630:2010

Guidance for evaluating exposure from multiple electromagnetic sources

National foreword

This Published Document is the UK implementation of IEC/TR 62630:2010.

The UK participation in its preparation was entrusted to Technical Committee GEL/106, Human exposure to low frequency and high frequency electromagnetic radiation.

A list of organizations represented on this committee can be obtained on request to its secretary.

This publication does not purport to include all the necessary provisions of a contract. Users are responsible for its correct application.

ISBN 978 0 580 67860 8

ICS 17.220.20; 33.050.10

Compliance with a British Standard cannot confer immunity from legal obligations.

This Published Document was published under the authority of the Standards Policy and Strategy Committee on 30 September 2010.

Amendments issued since publication

Amd. No.	Date	Text affected

IEC/TR 62630

Edition 1.0 2010-03

TECHNICAL REPORT

colour inside

Guidance for evaluating exposure from multiple electromagnetic sources

INTERNATIONAL
ELECTROTECHNICAL
COMMISSION

PRICE CODE X

ICS 17.220.20; 33.050.10

ISBN 2-8318-1083-8

CONTENTS

INTERNATIONAL ELECTROTECHNICAL COMMISSION

GUIDANCE FOR EVALUATING EXPOSURE FROM MULTIPLE ELECTROMAGNETIC SOURCES

FOREWORD

1) The International Electrotechnical Commission (IEC) is a worldwide organization for standardization comprising all national electrotechnical committees (IEC National Committees). The object of IEC is to promote international co-operation on all questions concerning standardization in the electrical and electronic fields. To this end and in addition to other activities, IEC publishes International Standards, Technical Specifications, Technical Reports, Publicly Available Specifications (PAS) and Guides (hereafter referred to as "IEC Publication(s)"). Their preparation is entrusted to technical committees; any IEC National Committee interested in the subject dealt with may participate in this preparatory work. International, governmental and non-governmental organizations liaising with the IEC also participate in this preparation. IEC collaborates closely with the International Organization for Standardization (ISO) in accordance with conditions determined by agreement between the two organizations.
2) The formal decisions or agreements of IEC on technical matters express, as nearly as possible, an international consensus of opinion on the relevant subjects since each technical committee has representation from all interested IEC National Committees.
3) IEC Publications have the form of recommendations for international use and are accepted by IEC National Committees in that sense. While all reasonable efforts are made to ensure that the technical content of IEC Publications is accurate, IEC cannot be held responsible for the way in which they are used or for any misinterpretation by any end user.
4) In order to promote international uniformity, IEC National Committees undertake to apply IEC Publications transparently to the maximum extent possible in their national and regional publications. Any divergence between any IEC Publication and the corresponding national or regional publication shall be clearly indicated in the latter.
5) IEC itself does not provide any attestation of conformity. Independent certification bodies provide conformity assessment services and, in some areas, access to IEC marks of conformity. IEC is not responsible for any services carried out by independent certification bodies.
6) All users should ensure that they have the latest edition of this publication.
7) No liability shall attach to IEC or its directors, employees, servants or agents including individual experts and members of its technical committees and IEC National Committees for any personal injury, property damage or other damage of any nature whatsoever, whether direct or indirect, or for costs (including legal fees) and expenses arising out of the publication, use of, or reliance upon, this IEC Publication or any other IEC Publications.
8) Attention is drawn to the Normative references cited in this publication. Use of the referenced publications is indispensable for the correct application of this publication.
9) Attention is drawn to the possibility that some of the elements of this IEC Publication may be the subject of patent rights. IEC shall not be held responsible for identifying any or all such patent rights.

The main task of IEC technical committees is to prepare International Standards. However, a technical committee may propose the publication of a technical report when it has collected data of a different kind from that which is normally published as an International Standard, for example "state of the art".

IEC/TR 62630, which is a technical report, has been prepared by IEC technical committee 106: Methods for the assessment of electric, magnetic and electromagnetic fields associated with human exposure.

The text of this technical report is based on the following documents:

Enquiry draft	Report on voting
106/173/DTR	106/196/RVC

Full information on the voting for the approval of this technical report can be found in the report on voting indicated in the above table.

This publication has been drafted in accordance with the ISO/IEC Directives, Part 2.

The committee has decided that the contents of this publication will remain unchanged until the stability date indicated on the IEC web site under "http://webstore.iec.ch" in the data related to the specific publication. At this date, the publication will be

- reconfirmed,
- withdrawn,
- replaced by a revised edition, or
- amended.

A bilingual version of this publication may be issued at a later date.

IMPORTANT – The 'colour inside' logo on the cover page of this publication indicates that it contains colours which are considered to be useful for the correct understanding of its contents. Users should therefore print this document using a colour printer.

INTRODUCTION

This Technical Report provides guidance to IEC TC 106 project teams on how to evaluate the combined exposures from multiple electromagnetic (EM) sources in the frequency range 100 kHz to 300 GHz when *specific absorption rate* (*SAR*) and *equivalent power density* (*S*) are the relevant exposure metrics, as defined by the main international guidelines recommending limits on human exposure to EM fields.

SAR and power density are energy-intensive exposure metrics related to tissue heating. Other metrics have been defined in some exposure guidelines to regulate different effects, e.g., electro-stimulation. Guidance on evaluating exposure from multiple EM sources based on these other exposure metrics requires separate further study

This Technical Report considers the combination of exposures from multiple EM sources

a) which reside on the same electronic device (e.g. multi-band mobile phone);
b) arising from multiple devices (e.g. multiple base station antennas);
c) arising from temporally uncorrelated fields (e.g., transmitters operating in different bands);
d) arising from temporally correlated fields (e.g., adaptive (beam-steering) antenna arrays).

Only intentional EM-energy transmitters are considered.

NOTE Evaluation of spurious radiation from non-intentional emitters is addressed in electromagnetic compatibility (EMC) standards dealing with unwanted EM emissions from electronic devices. The guidance in this Technical Report is not specifically intended for combining exposures from non-intentional radiating sources, such as EM leakages from electronic devices that are not designed for purpose of radiated RF emission. However, it may be possible to use some of the methods in this Technical Report to evaluate multiple exposures when some of the sources are not designed to radiate EM energy, e.g. microwave ovens or RF welders and dryers.

This Technical Report establishes basic, rigorous techniques to estimate accurately and conservatively the combined exposure from multiple EM sources. In developing International Standards, it is anticipated that IEC Project Teams may deviate from or further evolve these techniques as required to better address specific device or evaluation requirements.

The techniques established in this Technical Report allow summing internal fields for the purpose of determining *SAR* and external fields for determining the power density. They do not describe how to perform the volume or surface averaging procedures that would be required to derive the compliance metrics (e.g., 10-g *SAR* or spatially-averaged power density) most commonly employed in national or international exposure guidelines.

This Technical Report does not define any test method or algorithm to determine product compliance with exposure limits, leaving that task to product compliance standards. Even though an effort is made to provide guidance consistent with the most referenced international exposure guidelines, the Technical Report does not establish or imply any requirement to follow any specific national or international exposure guideline since that is a regulatory matter. Rather, imposition of requirements depends on the policy of national regulators.

GUIDANCE FOR EVALUATING EXPOSURE FROM MULTIPLE ELECTROMAGNETIC SOURCES

1 Scope

This Technical Report describes exposure evaluation concepts and techniques for the overall exposure level in spatial regions and occupants caused by the simultaneous exposure to multiple narrowband electromagnetic (EM) sources. Throughout this Technical Report, it is assumed that the exposure evaluation occurs under static conditions, i.e., the source position and transmit-mode characteristics (e.g. emitted power, modulation scheme, etc.) of the device(s) under test do not vary significantly over the time required to carry out the evaluation using the chosen evaluation technique (e.g., field measurements).

The vast majority of wireless communication systems worldwide employ signalling schemes featuring narrowband waveforms, hereinafter defined as signal waveforms occupying a frequency band not broader than 10 % of its central frequency (justification of this threshold is provided below). For information, Annex A presents the operating system bands and channel bandwidths of several common wireless services.

Wide-band communication systems, e.g., ultra-wideband (UWB) systems employing impulsive waveforms with fractional bandwidth well in excess of 10 %, are relatively new to the marketplace, have experienced limited deployment so far, and are not typically regarded as significant contributors to EM exposure levels due to low transmit power levels.

NOTE Present exposure evaluation standards for fixed or mobile wireless communication devices, e.g., IEC 62209-1, are mostly tailored towards defining suitable techniques for narrowband waveforms. For instance, they recommend the use of scalar E-field or H-field sensors, e.g., miniature diode-detector probes, which typically provide accurate readings for narrowband waveforms, as defined herein. The paucity of UWB wireless communication systems, which have only very recently been introduced in the marketplace, as well as the low power levels associated with the corresponding signals to avoid interfering with coexisting electronic systems, has so far reduced the priority to standardize suitable evaluation techniques and to develop the relevant test instrumentation.

2 Normative references

The following referenced documents are indispensable for the application of this document. For dated references, only the edition cited applies. For undated references, the latest edition of the referenced document (including any amendments) applies.

IEC 62209-1:2005, *Human exposure to radio frequency fields from handheld and body-mounted wireless communication devices – Human models, instrumentation, and procedures – Part 1: Procedure to determine the specific absorption rate (SAR) for hand-held devices used in close proximity to the ear (frequency range of 300 MHz to 3 GHz)*

3 Terms, definitions and abbreviations

For the purposes of this document, the following terms and definitions apply.

3.1 Terms and definitions

3.1.1
air-interface
access mode
the radio portion of the link between the mobile station and the active base station. In the context of the Open Systems Interconnection Reference Model, the air interface operates at the Physical Layer and the Data Link Layer

3.1.2
antenna
aerial (deprecated)
that part of a radio transmitting or receiving system which is designed to provide the required coupling between a transmitter or a receiver and the medium in which the radio wave propagates

NOTE 1 In practice, the terminals of the antenna or the points to be considered as the interface between the antenna and the transmitter or receiver should be specified.

NOTE 2 If a transmitter or receiver is connected to its antenna by a feed line, the antenna may be considered to be a transducer between the guided waves of the feed line and the radiated waves in space.

3.1.3
antenna array
an antenna comprised of a number of generally identical radiating elements, arranged, oriented and excited to obtain a prescribed radiation pattern enhancing radiation in one or more directions and reducing radiation in other directions

NOTE 1 Typical examples include vertical arrays used in panel antennas at RBS sites.

NOTE 2 In most cases radiating elements are identical and congruent by translation or by rotation about an axis; moreover they are in general regularly spaced.

NOTE 3 In French, unless otherwise specified, the use of the term "antenne en réseau" implies that radiating elements are congruent by a simple translation.

3.1.4
antenna array, adaptive
smart antenna
antenna system incorporating active circuits associated with radiating elements whereby one or more of the characteristics of the antenna are automatically modified in a prescribed manner as a function of the received signal or changes in the electromagnetic environment

NOTE Recently, the technology has been extended to use the multiple antennas at both the transmitter and receiver; such a system is called a multiple-input multiple-output (MIMO) system. As extended smart antenna technology, MIMO supports spatial information processing, which includes spatial information coding such as Spatial Multiplexing and Diversity Coding, as well as beamforming.

3.1.5
antenna field regions
classification of the important spatial subdivisions of an antenna electromagnetic field. The subdivisions, at non-uniquely defined distances from the antenna, include the reactive near-field region adjacent to the antenna, the radiating near-field region (for large antennas commonly referred to as the Fresnel region), a transition zone, and furthermost, the far-field region, also known as the Fraunhofer region. *See also*: **near-field region** and **far-field region**

3.1.6
antenna gain
ratio, generally expressed in decibels, of the radiation intensity produced by an antenna in a given direction to the radiation intensity that would be obtained if the power accepted by the antenna were radiated equally in all directions

NOTE 1 If no direction is specified, the direction of maximum radiation intensity from the given antenna is implied.

NOTE 2 If the antenna is lossless, its absolute gain is equal to its directivity in the same direction.

3.1.7
antenna, radiation pattern
spatial distribution of a quantity that characterizes the electromagnetic fields radiated by an antenna

NOTE The distribution can be expressed as a mathematical function or as a graphic representation. The quantities that are most often used to characterize the radiation from an antenna are proportional to, or equal to, power density, radiation intensity, directivity, phase, polarisation, and field strength.

3.1.8
antenna, reconfigurable beam
shaped-beam antenna designed so that some of its radiation characteristics, such as the radiation pattern, can easily be modified, for example by telecommand

3.1.9
antenna, steerable-beam
antenna in which the direction of the main lobe can be changed either by controlling the excitation of the different elements or by mechanical means other than moving the entire antenna

3.1.10
average (temporal) power
rate of radiated energy transfer over a given time interval ΔT, given by

$$\overline{P}_{\text{avg}}(t) = \frac{1}{\Delta T} \int_{t-\Delta T/2}^{t+\Delta T/2} P(\tau)\,\mathrm{d}\tau ,$$

where

ΔT is the (sliding) observation time window in seconds;

$P(t)$ is the instantaneous transmitted power in watts;

$\overline{P}_{\text{avg}}$ is the average (temporal) transmitted power over the interval ΔT in watts

NOTE The average power is a function of the time window ΔT, assuming a constant value only if $\Delta T \to \infty$.

3.1.11
average (temporal) power density
instantaneous power density integrated over a specific time duration. The time duration could be source related, e.g., the source repetition period, or use related, e.g., the averaging time specified in exposure guidelines. Average power density is expressed in units of watts per square metre (W/m^2)

NOTE In speaking of average power density in general, it is necessary to distinguish between the spatial average (at a given instant) and the time average (at a given point).

3.1.12
basic restriction
restrictions on human exposure to time-varying electric, magnetic, and electromagnetic fields that are based directly on the applicable national or international exposure guidelines

NOTE In the context of this Technical Report, applicable *specific absorption rate* (*SAR*) limits represent the basic restrictions.

3.1.13
beamforming (digital)
method used to create the radiation pattern of the antenna array by adding constructively the phases of the signals in the direction of the targets/mobiles desired, and nulling the pattern of the targets/mobiles that are undesired/interfering targets. This may be done adaptively by digital signal processors to provide optimal beamforming

3.1.14
co-located transmitters
transmitters located in close proximity to each other so they can be considered as occupying the same location

NOTE The distance under which two or more transmitters may be considered as "co-located" depends on their respective power and frequency, as well as on the evaluation area or volume of interest. "Co-location", a property describing in general the relative proximity of two or more objects, i.e. occupying together a single location, may have impact on the approach required to evaluate the overall exposure.

3.1.15
collinear array
an antenna consisting of a linear array of radiating elements, usually dipoles, with their axes lying in a straight line

3.1.16
complex (electric or magnetic) field envelope
a complex vector whose components are the complex envelopes of the electric or magnetic field components. For time-harmonic fields, the complex envelope reduces to the field phasor

3.1.17
conductivity, (equivalent electrical)
scalar or tensor quantity the product of which by the electric field strength in a medium is equal to the electric current density. The unit of conductivity is siemens per metre (S/m)

NOTE For an isotropic medium the conductivity is a scalar quantity; for an anisotropic medium it is a tensor quantity.

3.1.18
correlated waveforms (in time)
signal waveforms yielding non-zero time-domain correlation integral at some time instant. For two power-limited signals $s_1(t), s_2(t)$, said integral is defined as

$$(s_1 \otimes s_2)(t) = \lim_{T \to \infty} \frac{1}{2T} \int_{-T}^{+T} s_1(\tau)^{+} s_2(t+\tau)\, d\tau ,$$

where the superscript $+$ represents the complex conjugate operation.

NOTE This definition is mathematically convenient since it allows exploiting some useful analytical properties of correlation and convolution integrals but requires knowledge of the signal waveforms over an infinite time. Such a requirement may be impractical when performing exposure measurements. As discussed in Annex B, B.2 and B.3, when dealing with wireless communication waveforms that typically feature very large bit-rates due to high data throughputs and processing gains, signal correlation may be accurately characterized over a few seconds at most.

3.1.19
correlated fields (in time)
electromagnetic fields, associated to distinct signal waveforms, yielding non-zero time-domain correlation integral at some time instant. For two power-limited field distributions $\mathbf{F}_1(\mathbf{r},t), \mathbf{F}_2(\mathbf{r},t)$, said integral is defined as

$$\left(\mathbf{F}_1 \otimes \mathbf{F}_2\right)(\mathbf{r},t) = \lim_{T\to\infty} \frac{1}{2T} \int_{-T}^{+T} \mathbf{F}_1\left(\mathbf{r},\tau\right)^{+} \cdot \mathbf{F}_2\left(\mathbf{r},t+\tau\right) d\tau ,$$

where $\mathbf{r}$ is the location vector and the symbol $\cdot$ represents the inner product operation.

NOTE Observe that two fields are *uncorrelated* at locations where they are *geometrically orthogonal*. This property does not generally hold at nearby points unless the respective waveforms are uncorrelated (Annex B, B.2).

3.1.20
device
material element or assembly of such elements intended to perform a required function

NOTE In the context of this Technical Report, a device may comprise multiple EM sources.

3.1.21
dipole antenna
doublet
a symmetrical antenna composed of conductors usually rectilinear and energized by a balanced feed

NOTE The word "dipole" is sometimes used to describe antennas which do not conform in all respects to the above definition. In such cases, the word should be qualified, for example: "asymmetrical dipole". Common usage considers a dipole antenna to be a metal radiating structure that supports a line-current distribution similar to that of a thin straight wire, a half-wavelength long, so energized that the current has a node only at each end.

3.1.22
electric field strength
vector field quantity $\mathbf{E}$ which exerts on any charged particle at rest a force $\mathbf{F}$ equal to the product of $\mathbf{E}$ and the electric charge q of the particle

$$\mathbf{F} = q\,\mathbf{E} ,$$

where

$\mathbf{F}$ is the vector force acting on the particle in newtons;

q is the charge on the particle in coulombs;

$\mathbf{E}$ is the electric field in volts per metre.

3.1.23
(plane-wave) equivalent power density
the normalised value of the square of the electric or the magnetic field strength at a point. The value is expressed in W/m^2 and is computed in terms of the electric or magnetic field as follows:

$$S = \frac{|\,\mathbf{E}\,|_{rms}^2}{\eta_0} = \eta_0\,|\,\mathbf{H}\,|_{rms}^2$$

where η_0 is the free space wave impedance, approximately 377 Ω.

3.1.24
exposure evaluation
process of measuring or estimating the intensity, frequency (and duration of human exposure if required to compare with applicable exposure limits), field strength, power density or *SAR* associated with electromagnetic fields

3.1.25
exposure, partial-body
localised exposure of part of the body, producing a corresponding localised *SAR*, as distinct from a whole-body exposure

3.1.26
exposure, whole-body
exposure of the whole body

3.1.27
exposure quotient (EQ)
the evaluated exposure parameter related to the relevant compliance limit expressed as the energy-intensive fraction of the related limit at a given frequency

3.1.28
far-field region
that region of the time-harmonic field of an antenna where the angular field distribution is essentially independent of the distance from the antenna. In this region (also called the free-space region), the field has a spherical-wave character and, locally, a substantial plane-wave character, i.e., very uniform distributions of electric field strength and magnetic field strength in planes transverse to the direction of propagation. For larger antennas especially, the far-field region is also referred to as the Fraunhofer region

3.1.29
intended use
the reasonably foreseeable use of a device for the purpose intended, over its full range of applicable functions, in accordance with the instructions provided by the manufacturer, including instructions on installation, operating position and orientation

3.1.30
isotropic field sensor (probe)
electric field or magnetic field sensor whose response is independent of the polarisation and incidence angle of the incident waves

3.1.31
magnetic field strength
vector quantity $\mathbf{H}$ obtained at a given point by subtracting the magnetisation $\mathbf{M}$ from the magnetic flux density $\mathbf{B}$ divided by the magnetic constant μ_0:

$$\mathbf{H} = \frac{\mathbf{B}}{\mu_0} - \mathbf{M}$$

where

$\mathbf{B}$ is the magnetic flux density in teslas; a vector field quantity which exerts on any charged particle q having velocity $\mathbf{v}$ a force $\mathbf{F} = q(\mathbf{v} \times \mathbf{B})$;

μ_0 is the magnetic constant (permeability) in henries per metre;

$\mathbf{M}$ is the magnetisation in amperes per metre; for the purposes of this document, we shall assume $\mathbf{M} = \mathbf{0}$ in exposed tissues and in air;

$\mathbf{H}$ is the magnetic field in amperes per metre

3.1.32
multiple-input and multiple-output (MIMO)
the use of multiple antennas at both the transmitter and receiver to improve communication performance. It is one of several forms of smart antenna technology

3.1.33
multi-band (transmitter or device)
a transmitter or device capable of operating in more than one frequency band

3.1.34
multi-mode (transmitter or device)
a transmitter or wireless device capable of operating in more than one air-interface, e.g., UMTS, GSM and WLAN

3.1.35
narrowband electromagnetic source
source of electromagnetic field emissions whose occupied bandwidth is 10 % or less than its centre frequency

NOTE The terms narrowband, broadband, ultra-wideband have been used with different meanings and interpretations for different wireless products, technologies and markets. Therefore, the present definition is explicitly intended to be applicable within the context of this Technical Report.

3.1.36
near-field region
a region in the time-harmonic field of an antenna, located near the antenna, in which the electric and magnetic fields do not have a substantially plane-wave character, but vary considerably from point to point

NOTE The term is only vaguely defined and has different meanings for large and small antennas. It is further subdivided into the reactive near-field region, which is closest to the antenna and contains most or nearly all of the stored energy associated with the field of the antenna, and the radiating near-field region. If the antenna has a maximum overall dimension that is not large compared with the wavelength, the radiating near-field region may not exist. For antennas large in terms of wavelength, the radiating near-field region is sometimes referred to as the Fresnel region on the basis of analogy to optical terminology.

3.1.37
occupied bandwidth
width of the occupied band of an emission

3.1.38
peak spatial-average *SAR*
the maximal value of the local *SAR* averaged over a specified volume or mass, e.g., any 1 g or 10 g of tissue in the shape of a cube. *SAR* is expressed in units of watts per kilogram (W/kg)

3.1.39
phantom, (head or torso)
in the context of this Technical Report, a simplified representation or a model similar in appearance to the human (head or torso) anatomy and composed of materials with electrical properties similar to the corresponding tissues

3.1.40
point source
source of radiation the dimensions of which are small enough, compared with the distance between the source and the irradiated surface, for them to be neglected in calculations and measurements

NOTE A point source which emits uniformly in all directions is called an isotropic or uniform point source.

3.1.41
polarisation (of a wave or field vector)
the property of a sinusoidal electromagnetic wave or field vector defined at a fixed point in space by the direction of the electric field strength vector or of any specified field vector; when this direction varies with time the property may be characterized by the locus described by the extremity of the considered field vector

3.1.42
power
a physical quantity describing the rate of delivery or transmission of energy. In this document, power will refer to radio frequency power with units of watts (W)

3.1.43
power (flux) density
the power passing through an element of surface normal to the direction of propagation of energy of an electromagnetic wave divided by the area of the element, usually expressed in watts per metre squared (W/m^2). *Also referred to as* **radiant flux density**

3.1.44
radio communication base station (RBS)
fixed equipment including the radio transmitter and associated antenna(s) as used in wireless telecommunications networks

3.1.45
radio frequency (RF)
the frequency in the portion of the electromagnetic spectrum that is between the audio-frequency portion and the infrared portion

NOTE The present practicable limits of radio frequency are roughly 10 kHz–300 GHz. Within this frequency range, electromagnetic radiation may be detected and amplified as an electric current at the wave frequency.

3.1.46
reactive field
electric and magnetic fields surrounding an antenna or other electromagnetic devices that result in storage rather than propagation of electromagnetic energy

3.1.47
root-mean-square (r.m.s.) value
for a time-dependent quantity, positive square root of the mean value of the square of the quantity taken over a given time interval ΔT . *Also referred to as* **effective value**. For a complex quantity *z* depending on a real variable *t*, the r.m.s. value of the magnitude of *z* is:

$$\left|z_{rms}(t)\right|_{rms} = \sqrt{\frac{1}{\Delta T}\int_{t-\Delta T/2}^{t+\Delta T/2}\left|z(\tau)\right|^2 d\tau} \quad .$$

NOTE 1 For a periodic quantity, the time interval comprises an integral number of periods.

NOTE 2 For a sinusoidal quantity A cos(ω t + θ), the r.m.s. value is A/ √2.

3.1.48
scalar field sensor (probe)
in the context of this Technical Report, an isotropic probe providing readings of the magnitude of the field components, or a single reading of the field magnitude

3.1.49
source, electromagnetic (EM)
in the context of this Technical Report, the ensemble of physical transducers (e.g., RF mixers, transmission lines, power amplifiers, filters, antennas) inside a wireless communication device that transpose a suitably encoded and modulated signal carrying communication information into radiated EM waves emanating from the device. *Also referred to as* **transmitter**

3.1.50
spatial average
as applied to the measurement of electric or magnetic fields for the assessment of whole-body exposure means the root mean square of the field over a suitably defined area. The spatial average can be measured by scanning a suitable measurement probe

3.1.51
specific absorption rate (*SAR*)
the time derivative of the incremental electromagnetic energy (dW) absorbed by (dissipated in) an incremental mass (dm) contained in a volume element (dV) of given mass density (ρ):

$$SAR = \frac{d}{dt}\left(\frac{dW}{dm}\right) = \frac{d}{dt}\left(\frac{dW}{\rho dV}\right).$$

SAR can be obtained using the following expression:

$$SAR = \frac{\sigma}{\rho} |\mathbf{E}|^2_{rms} ,$$

where

$|\mathbf{E}|_{rms}$ is the r.m.s. value of the electric field strength in the tissue in volts per metre;

σ is the electric conductivity of the tissue in siemens per metre;

ρ is the density of the tissue in kilograms per cubic metre;

SAR is the specific absorption rate in watts per kilogram.

3.1.52
vector field sensor (probe)
in the context of this Technical Report, an isotropic probe providing readings of the magnitude and the phase for each the field component

3.1.53
wavelength
distance in the direction of propagation of a periodic wave between two successive points at which the phase is the same. The wavelength λ is related to the magnitude of the phase velocity v_p and the frequency f by the equation:

$$\lambda = \frac{v_p}{f}.$$

The wavelength λ of an electromagnetic wave is related to the frequency and speed of light in the medium by the expression:

$$c = f\lambda,$$

where:

f	is the frequency in hertz;
c	is the speed of light in metres per second;
λ	is the wavelength in metres.

NOTE In free space the velocity of an electromagnetic wave is equal to the speed of light in vacuo. The wavelength in a medium is equal to the wavelength in vacuo divided by the refractive index of the medium. Unless otherwise stated, values of wavelength are generally those in air.

3.2 Physical quantities

The internationally accepted SI-units are used throughout this Technical Report.

Symbol	**Quantity**	**Unit**	**Dimensions**
E	electric field strength	volt per metre	V m^{-1}
f	frequency	hertz	Hz
H	magnetic field strength	ampere per metre	A m^{-1}
$\overline{P}_{avg}$	average (temporal) power	watt	W
SAR	specific absorption rate	watt per kilogram	W kg^{-1}
S	(plane-wave) equivalent power density	Watt per square metre	W m^{-2}
ε	dielectric permittivity	farad per metre	F m^{-1}
λ	wavelength	metre	m
μ	magnetic permeability	henry per metre	H m^{-1}
ρ	mass density	kilogram per cubic metre	Kg m^{-3}
σ	(equivalent) electrical conductivity	siemens per metre	S m^{-1}

3.3 Constants

Symbol	**Physical constant**	**Magnitude**
c	speed of light in vacuo	$2{,}9979 \times 10^{8}$ m s^{-1}
η_0	impedance of free space	376,73 Ω
ε_0	permittivity of free space	$8{,}8542 \times 10^{-12}$ F m^{-1}
μ_0	permeability of free space	$4\,\pi \times 10^{-7}$ H m^{-1}

3.4 Abbreviations

(N)AMPS	(Narrowband) Advanced Mobile Phone System
BCCH	Broadcast Control Channel
CDMA	Code Division Multiple Access
D-AMPS	Digital Advanced Mobile Phone System
DECT	Digital Enhanced Cordless Telecommunications

EM	Electromagnetic
FDTD	Finite-Difference Time-Domain
FEM	Finite Element Method
GSM	Global System for Mobile communications (originally *Groupe Spécial Mobile*)
JTACS	Japanese Total Access Communication System
LTE	Long Term Evolution
MIMO	Multiple-Input and Multiple-Output
MoM	Method of Moments
NFC	Near Field Communication
PDC	Personal Digital Cellular
PHS	Personal Handy-phone System
RBS	Radio Communication Base Station
RF	Radio Frequency
r.m.s., rms	Root Mean Square
SAR	Specific Absorption Rate
(E)TACS	(Extended) Total Access Communication System
TETRA	Trans-European Trunked RAdio
UMTS	Universal Mobile Telecommunications System
UWB	Ultra Wide Band
Wi-Fi	Wireless Fidelity
WiMAX	Worldwide Inter-operability for Microwave Access
WLAN	Wireless Local Area Network
TV	Television

3.5 Vector notations

Throughout this Technical Report, space-time domain vectors are indicated by lowercase bold symbols (e.g., $\mathbf{e}(\mathbf{r},t)$ for the electric field) and the relative complex envelopes by uppercase bold characters (e.g., $\mathbf{E}(\mathbf{r},t)$). The corresponding components are indicated by italicized lowercase (e.g., $e_w(\mathbf{r},t), w = x, y, z$) and uppercase (e.g., $E_w(\mathbf{r},t)$) symbols, respectively.

4 Overview

Exposure from multiple EM sources is quite common, particularly in the case of simultaneous exposure from multiple broadcast and cellular infrastructure transmitters. For instance, urban and suburban areas are typically covered by broadcast services, e.g., radio and TV, as well as by mobile communication services, e.g., mobile telephony, public safety and emergency systems. Exposure levels from these kinds of sources, at locations where people would normally reside, are typically orders of magnitude lower than the main international exposure guideline limits. The respective frequency bands are typically disjointed, thus the corresponding signal waveforms are *uncorrelated* (see Subclause 6.2), and the overall exposure may be readily determined by a suitable summation of the individual exposure contributions expressed in terms of energy-intensive quantities, e.g., power density.

Over the last few years combined data and voice communication systems, e.g., UMTS and WiMAX, have been deployed. There is also a growing number of personal communication devices that allow simultaneous transmission over multiple air-interfaces while being operated near the user's body. In most cases, multiple transmitters in portable wireless communicators operate in distinct frequency bands, e.g., GSM and Bluetooth, so the overall exposure can be determined by summing the corresponding *SAR* distributions. *SAR* summation is also legitimate when waveforms that operate in the same band, e.g., Wi-Fi and Bluetooth, are uncorrelated in time (see Subclause 6.4 and Annex B).

Lately, adaptive antenna arrays (also referred to as *smart antennas*) featuring beamforming (also called *beam-steering*) techniques are being deployed to increase system reliability and data throughput. These systems result in exposure from multiple *correlated* EM sources, featuring time-varying magnitude and phase relationships, so they require suitable yet practical exposure evaluation methods to address the additional complexity. This added complexity is illustrated in Figure 1 which shows a dual-panel antenna configuration.

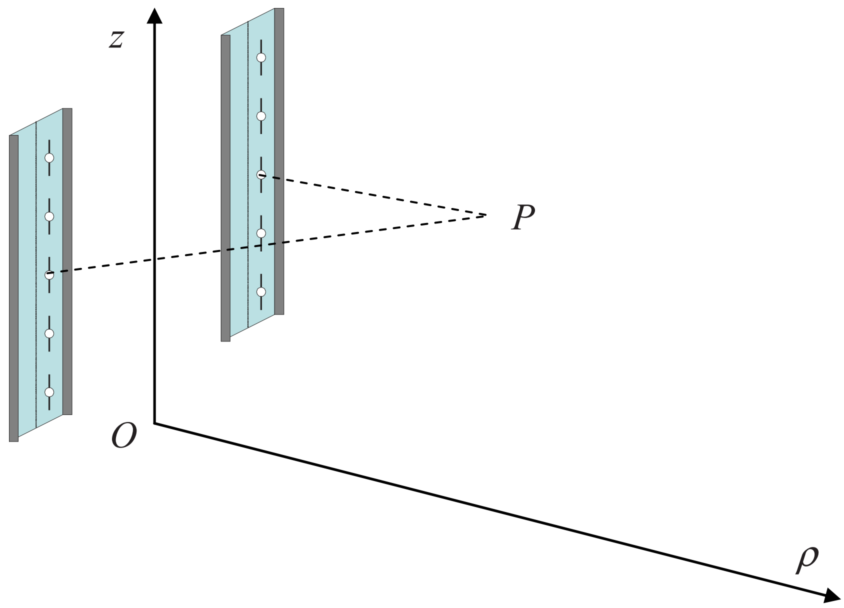

Figure 1 – Electrical paths from the radiating elements of each panel in a dual-panel antenna system to a field-point P on the ρ-z symmetry plane

In a conventional antenna system, both antennas radiate the same waveform with a constant magnitude and phase relationship, e.g., same magnitude and phase. In this instance, the respective electric fields would add in-phase everywhere on the symmetry plane ρ-z since any point (P) on the plane features the same electrical distance from each antenna.

In a beamforming smart antenna system, the magnitude and phase relationships are not constant but rather vary adaptively in real-time to enhance overall system performance. The respective fields on the symmetry plane, and by extension at any point in space, may have arbitrary phase and magnitude relationship at the time the measurement is performed. For instance, as intuitively illustrated in Figure 2, at measurement time (t) the respective fields (identified by the complex field envelopes $\mathbf{E}_1, \mathbf{E}_2$, analogues of the phasors for time-harmonic fields, see Annex B, B.1) may have the same magnitude but opposite phase so the resultant field envelope ($\mathbf{E}_1 + \mathbf{E}_2$) vanishes, while at another time ($t+\Delta t$) the fields may combine to produce a non-vanishing resultant field. It may be argued – though it is difficult to prove – that increasing measurement times would eventually allow capturing the peak combined exposure.[1] However, extending the measurement time at every evaluation point is likely to be impractical in some cases, for instance the battery of a portable device under test that incorporates a MIMO antenna system may not last long enough.

1 National or international exposure guidelines may include provisions for the time-averaging of the exposure. Therefore the peak instantaneous exposure may not necessarily represent the proper exposure metric to be used in associated compliance evaluations.

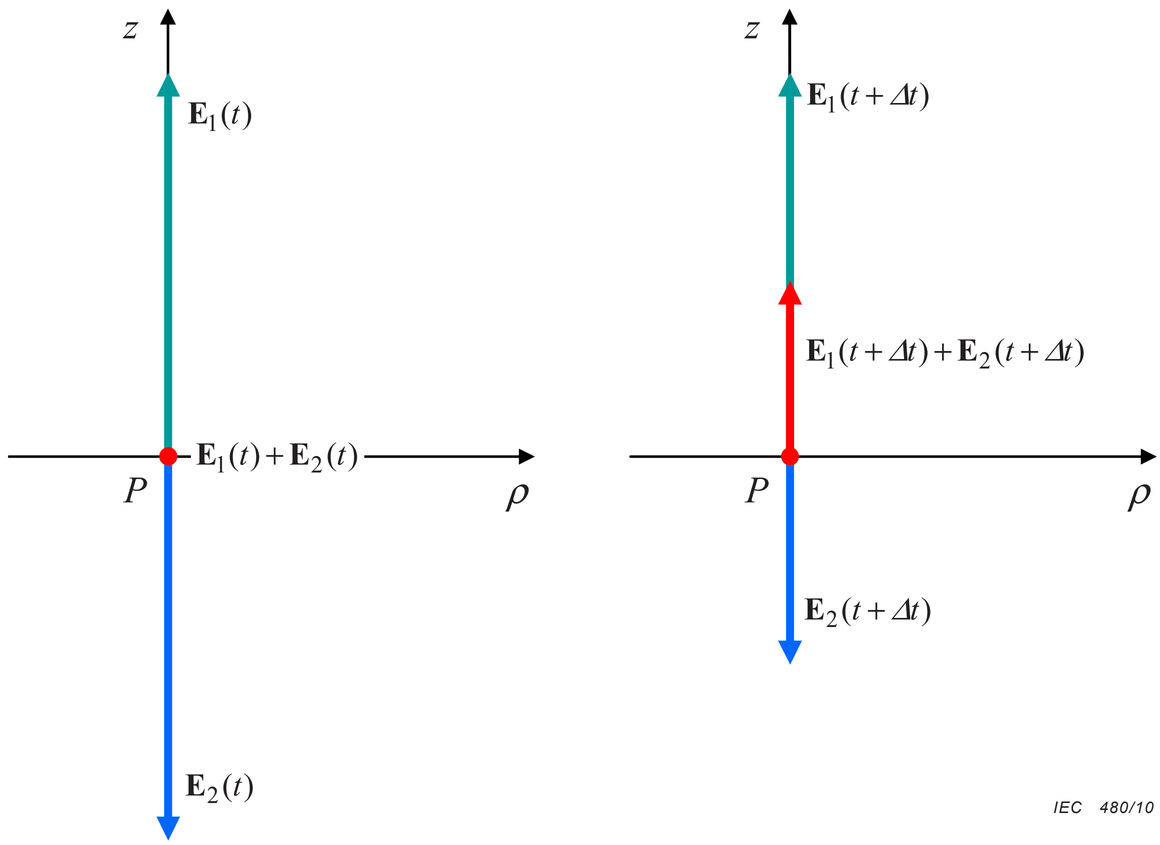

Figure 2 – True vector sum of the complex field envelopes produced at the field-point *P* by the individual antenna panels in Figure 1 at two different measurement times

This Technical Report is structured as follows. In Clause 5, a source classification is introduced to help differentiate between different kinds of devices, based on their intended operation and some intrinsic characteristics of their transmitters. Although such a classification may not be comprehensive, it includes most common wireless devices in the marketplace today.

The combined exposure evaluation techniques are thoroughly illustrated in Clause 6, with the relevant analytical details relegated to Annex B. For the reader's convenience, general guidance on the use of these techniques is synthetically provided in Subclause 6.1 before going into the corresponding analytical definitions. After illustrating the distinction between correlated and uncorrelated waveforms (Subclause 6.2), the relevant exposure metrics (*SAR* and equivalent power density) are defined in a suitable analytical format in Subclause 6.3 to facilitate the subsequent derivation of the corresponding combined evaluation techniques.

The case of uncorrelated EM sources is analysed first (Subclause 6.4 and Annex B), showing the legitimacy of the straightforward summation of *SAR* or power density distributions.

In contrast, the accurate combination of exposures from correlated EM sources with varying amplitude relationships generally requires the evaluation and vector summation of the individual fields at every evaluation point, as illustrated in Subclause 6.5. Whereas this is readily accomplished when EM simulations are possible (e.g., using the MoM, FEM, or FDTD methods), it can be onerous and excessively complex when measurements are the method of choice. Therefore, it may be desirable to resort to alternative methods yielding conservative estimates of the overall exposure while also preserving the option to employ the more conventional scalar measurement techniques and associated equipment.

To this purpose, this Technical Report presents alternative techniques to estimate conservatively the upper bound of the true field vector sum, which are practical and avoid the need for excessively long or onerous measurements (see 6.5.2 and Annex B). Their aim is to produce a conservative yet realistic exposure evaluation for correlated waveforms in smart antenna systems, i.e., to estimate conservatively the peak realised exposure at every evaluation point. The presented techniques allow the use of broadband or narrowband scalar field sensors rather than more complex and expensive vector sensors. The trade-off required to take advantage of these simpler, faster, and presumably more cost-efficient evaluation techniques is represented by the degree of exposure overestimation they introduce.

Various examples illustrating some possible applications of the aforementioned techniques are provided in Annex C. The combination of *SAR* distributions produced by GSM and Wi-Fi transmitters on a mobile handset is discussed in Annex C, C.2.1, while the exposure combination from a multi-antenna RBS site is illustrated in Annex C, C.2.2. Finally, an example illustrating the application of the rigorous and alternative techniques to correlated sources (the individual column arrays of a WiMAX panel antenna) is presented in Annex C, C.3.1, showing the moderate degree of overestimation that may be introduced by these alternative techniques.

5 Classification of devices and EM sources

5.1 General aspects

The landscape of wireless communication applications is rapidly expanding, and so is the variety of associated communication devices, both fixed and portable. Therefore, there may be many different EM source classification approaches. One possible approach, which may be helpful in dealing with exposure from multiple EM sources, is outlined below based on the notion that a wireless communication device may in general incorporate multiple transmitters (EM sources), thus classifications are provided for *devices* as well as *transmitters*.

5.2 Device classification based on the intended use: user-centric versus node-centric

Presently, IEC standards tend to differentiate between devices intended to be operated near the user’s head or body (i.e., providing a wireless communication service to a specific user and commonly including some form of user interface) and devices that provide an area of RF coverage (i.e., operating irrespective of a user’s body proximity). Examples of the former are GSM phones, portable 2-way radios, UMTS-enabled laptop computers, and many other devices in the scope of the IEC 62209-1 and 62209-2 standards. The latter include cellular RBS antennas, broadcast TV or FM radio antennas, Wi-Fi access points, as well as many other devices within the scope of the IEC 62232 standardization activities.

Therefore, a first-level classification may differentiate between devices intended for operation near the head or the body, which may be called *user-centric*, and devices intended for operation away from the body (a 20 cm threshold distance is currently defined in several IEC standards), which may be called *node-centric* to reflect their role in wireless networks. In general, electromagnetic exposure from user-centric devices is anticipated and designed for, whereas it is incidental to operation for node-centric ones.

Electromagnetic exposure from *multiple devices* has distinct characteristics depending on the device class, for instance:

a) Consider the user of a GSM phone employing a Bluetooth headset. The user is concurrently exposed by the RF energy emitted by the mobile phone and the headset. However, the mobile phone may be worn at the belt while the headset is worn at the head; therefore each device produces a localised exposure in distinct areas of the body (*partial-body exposure*), each not contributing to the localised exposure from the other. One device, the mobile phone, has multiple EM sources (GSM and Bluetooth transmitters); the other device, the headset, has only the Bluetooth transmitter. So, even though the user is exposed to the RF energy emitted by three RF transmitters in two separate devices, only the mobile phone requires a combined exposure evaluation.

b) Now consider a bystander being exposed by multiple RBS antennas aimed at different sectors, or belonging to different antenna masts, as sketched in Figure 3. Suppose that each antenna operates in both GSM bands (900 MHz and 1 800 MHz). Because the whole body is exposed far from the antennas (*whole-body exposure*), the exposure levels from all antenna transmitters need to be combined. In the example of Figure 3, a total of six signals over two frequency bands from three antennas contribute significantly to the overall exposure level at the location labelled "**X**". Observe that the exposure from each antenna field may consist of the superposition of direct and scattered waves, e.g. in highly reverberating environments such as urban settings. The field combination methods outlined in the following are applicable to these scenarios once the proper evaluation techniques, defined in applicable standards, are used for each antenna field evaluation.

In summary, when dealing with localized exposures produced by several user-centric devices hosting multiple EM sources, the exposure from each device may be evaluated independently when the cross-contributions to the individual *SAR* distributions can be reasonably neglected. In contrast, evaluating the exposure from node-centric devices may require that exposure from all concurrent sources be considered; therefore, determination of cross-contributions for node-centric devices represents a site or installation consideration.

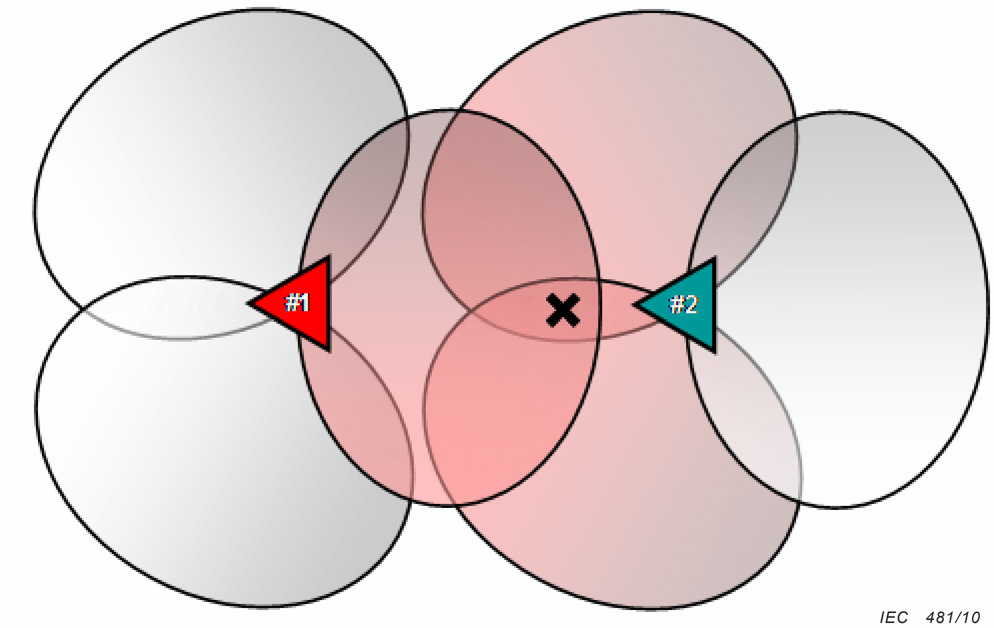

Figure 3 – Simultaneous exposure at the location X by multiple sector-antennas belonging to adjacent tri-sector cellular masts (labelled #1 and #2)

5.3 EM source classification: single-channel versus band-wide transmitters

Differences in the type of transmitters associated with the device classes defined above allow further divisions into sub-classes. During a voice conversation, the GSM transmitter in the mobile phone of the previous example operates in a single channel within its allocated GSM band (which includes a large number of communication channels), occasionally switching channel due to hand-offs between cells or to otherwise improve communication quality. Therefore, the GSM and Bluetooth signals emitted by the mobile phone are both narrowband, as illustrated in Table A.1, thus falling within the scope of this Technical Report and the applicability range of the field summation techniques outlined in Clause 6. In particular, the corresponding *SAR* distributions can be measured individually with high precision using conventional broadband scalar probes such as those recommended in IEC 62209-1.

Now consider the signals emitted by the dual-band cellular base station antennas described in 5.2 b), occupying the GSM 900 MHz and GSM 1800 MHz downlink bands. Within each band, the antennas emit a composite waveform formed by a number of signals corresponding to the active channels that at a given moment in time support the actively engaged mobile terminals. It should be evident that the signals emitted by these antennas are quite different from those emitted from the mobile phone in the previous example. In particular, over the typical measurement time they typically involve many concurrent channels occupying a significant portion if not the entire allocated band. As shown in Table A.1, most of these composite waveforms are still considered narrowband according to the definition adopted herein (Clause 1). However, measuring the maximum exposure to be expected from the aforementioned composite waveforms is no trivial task since the number and power level of the active channels change rapidly in time when, as customary, the exposure evaluation is carried out without interrupting the operating communication service. Consequently, the measurements cannot be carried out using broadband scalar probes but require vector probes and either narrowband or digital correlator receivers. For instance, the Broadcast Control Channel (BCCH) in GSM networks operates a constant power, so its exposure level may be measured with an antenna and a spectrum analyzer and then scaled up by the number of channels available at the RBS. Similarly, the exposure level by the *pilot channel* in CDMA networks, which also emits at constant power with a known Walsh code, may be measured with a digital correlator receiver and scaled up.

NOTE 1 Observe that broadband isotropic scalar field probes, e.g., those based on diode-detector technology (e.g., see IEEE Std C95.3-2002), are indeed suitable to monitor *actual* exposure levels from RBS antennas, i.e., when *peak* exposure evaluation is not needed. They are also suitable when it is known that all channels are set at maximum power levels. Typically, broadband scalar probes are very reliable for single-channel transmitters (e.g., mobile radios with vehicle-mounted antennas). However, they may not necessarily be suitable for band-wide transmitters should the operating system bandwidth be very broad, as in systems hosting very large numbers of communication channels. The reason why the 10 % fractional bandwidth threshold was defined for narrowband waveforms in the scope of this Report was to limit its applicability to cases for which commonly employed exposure evaluation techniques *and* associated technologies are expected to be accurate. Also observe that most of the common wireless services listed in Table A.1 have band-wide fractional bandwidths that fall within said threshold.

Based on the foregoing, a subdivision in sub-classes of sources, those emitting signals over individual channels of the respective allocated service bands (*single-channel transmitters*), and those emitting simultaneously multiple signals over several channels in the bands (*band-wide transmitters*), may be meaningful particularly for node-centric devices. In the former case, peak exposure may be evaluated using conventional broadband scalar probes when the signal power is set to or known to be at its maximum level, while in the latter case peak exposure evaluations may require the use of narrowband receivers or digital correlator detectors. Examples of devices falling in the classes defined above are listed in Table 1.

Table 1 – Source classes: characteristics and examples of source classification

		INTENDED USE		PEAK-EXPOSURE MEASUREMENT TECHNIQUE
		USER-CENTRIC	NODE-CENTRIC	
TRANSMITTER	SINGLE-CHANNEL	Mobile phone Professional 2-way radio	Wi-Fi access point RF beacon	BROADBAND SCALAR/VECTOR
	BAND-WIDE	-	GSM RBS antenna TV repeater station	CORRELATOR/ NARROWBAND
EXPOSURE CROSS-CONTRIBUTION [2]		TYPICALLY NEGLIGIBLE	POTENTIALLY NON-NEGLIGIBLE	

NOTE 2 The above classification illustrates the applicability of the exposure combination approaches outlined in Clause 6 and is intended to provide useful guidance in their application. Although such a classification covers a broad range of devices and transmitters, it should not be regarded as covering any possible present or future ones.

NOTE 3 Determination of whether evaluation of the combined simultaneous exposure from user-centric and node-centric devices is required represents a regulatory matter.

2 Transmitter co-location is frequently the factor that determines whether cross-contributions need to be evaluated.

6 Combined exposure from multiple narrowband EM sources

6.1 Guidance on the selection of the exposure summation approach

Table 2 provides a summary of the various approaches to evaluate the combined exposure from multiple EM sources outlined in the following subclauses, and includes guidance about the experimental or analytical/computational techniques that may be required to apply each approach.

Table 2 – Guidance on the selection of suitable evaluation techniques

<table>
<tr><th colspan="2">Evaluation Method</th><th>Uncorrelated signals</th><th>Correlated signals</th></tr>
<tr><td rowspan="4">MEASUREMENTS</td><td rowspan="2">SINGLE-CHANNEL TRANSMITTER</td><td rowspan="2">Broadband scalar probes
(SAR, S)
Equations (4)-(5)</td><td>Vector probes
($\boldsymbol{E}$, $\boldsymbol{H}$)
Equation (6)</td></tr>
<tr><td>Scalar probes
(SAR, S)
Equations (9)-(10) or (11)-(12)</td></tr>
<tr><td rowspan="2">BAND-WIDE TRANSMITTER</td><td rowspan="2">Narrowband/correlator scalar probes
(SAR, S)
Equations (4)-(5)</td><td>Narrowband/correlator
Vector probes
($\boldsymbol{E}$, $\boldsymbol{H}$)
Equation (6)</td></tr>
<tr><td>Narrowband/correlator
Scalar probes
(SAR, S)
Equations (9)-(10) or (11)-(12)</td></tr>
<tr><td rowspan="6">COMPUTATIONS</td><td rowspan="4">NUMERICAL SIMULATIONS</td><td rowspan="2">Full-wave EM simulations
(SAR, S)
Equations (4)-(5)</td><td>Full-wave EM simulations
($\boldsymbol{E}$, $\boldsymbol{H}$)
Equation (6)</td></tr>
<tr><td>Vector ray-tracing methods
($\boldsymbol{E}$, $\boldsymbol{H}$)
Equation (6)</td></tr>
<tr><td rowspan="2">Scalar ray-tracing methods
(S)
Equation (5)</td><td>Scalar ray-tracing methods
(S)
Equations (9)-(10)</td></tr>
<tr><td>Vector ray-tracing methods
($\boldsymbol{E}$, $\boldsymbol{H}$)
Equations (11)-(12)</td></tr>
<tr><td rowspan="2">FORMULAE</td><td rowspan="2">Scalar formulae
(SAR, S)
Equations (4)-(5)</td><td>Vector formulae
($\boldsymbol{E}$, $\boldsymbol{H}$)
Equation (6)</td></tr>
<tr><td>Scalar formulae
(SAR, S)
Equations (9)-(10)</td></tr>
</table>

NOTE 1 Table 2 should not be interpreted as limiting the options of available evaluation techniques, as other techniques may be demonstrated to be suitable to implement the approaches defined in Equations (4) to (12).

NOTE 2 Determining the combined exposure from multiple sources may involve the application of different techniques to different sources, and the suitable superposition of the corresponding results. For instance, combining the exposure of GSM (900 MHz) and NFC (13 MHz) signals from a mobile phone could in principle be performed by measuring and then superposing the respective *SAR* distributions over a common grid of points using Equation (4). However, measuring *SAR* at 13 MHz – a frequency that falls outside of the scope of IEC 62209-1 – may pose significant practical challenges (unique tissue-simulating liquids, unique E-field probes and unique probe calibration methods). Electromagnetic simulations may therefore provide suitable means to determine the NFC exposure by allowing the computation of the corresponding *SAR* distribution to be used in Equation (4).

6.2 Correlation between signals emitted by different EM sources

Consider different transmitters generating individual real signals ($s_k(t), k = 1, 2, \cdots$), that can be either correlated or uncorrelated in time (t). Two *uncorrelated*, real-valued signals identified by subscripts i and j, would feature a vanishing correlation integral, defined as follows:

$$\left(s_i \otimes s_j\right)(t) = \lim_{T \to \infty} \frac{1}{2T} \int_{-T}^{+T} s_i(\tau)^+ s_j(t+\tau)\, d\tau \equiv 0, \tag{1}$$

whereas *correlated* waveforms would exhibit non-zero correlation at some time instant.

In Annex B, B.2 it is shown that waveforms occupying disjoint bands are necessarily uncorrelated in time. This case is particularly important since in many practical instances multiple EM sources contributing to the exposure operate in different bands (e.g., GSM and Wi-Fi). However, there are other instances where different sources share the same operating band. In this case, the waveforms may be correlated or uncorrelated depending on the specific air-interface signalling characteristics, as discussed in Annex B, B.2.2. For instance, CDMA waveforms sharing the same band are uncorrelated if they employ orthogonal Walsh sequences to encode the information.

6.3 Relevant exposure metrics

Many national and international exposure guidelines identify the *specific absorption rate* (*SAR*) and the *plane-wave-equivalent power density* (*S*) as the relevant exposure metrics in the frequency range 100 kHz to 300 GHz. Even though *SAR* describes energy dissipation inside exposed bodies while power density refers to fields in air, they both are quantities related to the squared r.m.s. value of the electric field $\mathbf{e}(\mathbf{r}, t)$ at the generic field-point $\mathbf{r} = \hat{\mathbf{x}}\, x + \hat{\mathbf{y}}\, y + \hat{\mathbf{z}}\, z$ as follows:

$$SAR(\mathbf{r}) = \frac{\sigma(\mathbf{r})}{\rho(\mathbf{r})} \left|\mathbf{e}(\mathbf{r})\right|_{rms}^2 = \frac{\sigma(\mathbf{r})}{2\rho(\mathbf{r})} \left|\mathbf{E}(\mathbf{r})\right|_{rms}^2, \tag{2}$$

$$S(\mathbf{r}) = \frac{1}{\eta_0} \left|\mathbf{e}(\mathbf{r})\right|_{rms}^2 = \frac{1}{2\eta_0} \left|\mathbf{E}(\mathbf{r})\right|_{rms}^2, \text{[3]} \tag{3}$$

where $\sigma(\mathbf{r})$, $\rho(\mathbf{r})$ are the tissue conductivity and density distributions, respectively, $\mathbf{E}(\mathbf{r}, t)$ is the field complex envelope (see Annex B, B.3), and η_0 is the free-space wave impedance. [4]

---

3 The equivalent power density (S) may also be computed from the magnetic field by evaluating $|\mathbf{h}|_{rms}$; for brevity and without loss of generality, only the electric field dependence is used in the subsequent derivations.

4 Some guidelines define exposure limits in terms of plane-wave- equivalent electric or magnetic field magnitudes rather than power density. All the considerations regarding power density summation presented in this Report may be applied to r.m.s. field limits using the following substitutions: $|\mathbf{e}|_{rms} = \sqrt{\eta_0 S}$, $|\mathbf{h}|_{rms} = \sqrt{S / \eta_0}$.

NOTE 1 Equations (2) and (3) define point quantities, before performing any spatial averaging that may required in compliance evaluations. Spatial averaging techniques may be applied after the *SAR* or power density distribution is suitably determined.

NOTE 2 The *SAR* expression in Equation (2) is valid under the hypothesis that the tissue conductivity variation over the signal waveform bandwidth can be neglected, which is reasonably achieved over narrow frequency ranges. This limitation further justifies the signal fractional bandwidth limitation (10 %) adopted in this Technical Report.

6.4 Combined exposure from uncorrelated EM sources

The case of uncorrelated sources is the most common one when dealing with combined exposure from N electromagnetic sources, allowing the straightforward summation of *SAR* or power density distributions to yield the total exposure (see Annex B, B.4):

$$SAR_T(\mathbf{r}) = \sum_{k=1}^{N} SAR_k(\mathbf{r}), \tag{4}$$

$$S_T(\mathbf{r}) = \sum_{k=1}^{N} S_k(\mathbf{r}). \tag{5a}$$

NOTE 1 Equation (5a) may not necessarily represent the exposure metric when frequency-dependent power density limits [$S_{\lim}(f)$] apply, as required by some international exposure guidelines. In this case, the summation may be expressed in terms of *exposure quotients* to account for the frequency-dependent limits:

$$EQ_T(\mathbf{r}) = \sum_{k=1}^{N} EQ_k(\mathbf{r}) = \sum_{k=1}^{N} \frac{S_k(\mathbf{r})}{S_{\lim}(f_k)} \tag{5b}$$

f_k being the mid-band frequencies of the narrowband signals $s_k(t), k = 1 \cdots N$.

NOTE 2 Equations (4) and (5) allow the use of scalar (e.g., diode-detector based) E-field probes, which are already extensively employed for evaluating RF exposure from single-transmitter products. Therefore, from a practical viewpoint, implementing evaluation procedures for uncorrelated narrowband waveforms is not likely to require significant equipment upgrades or added complexity in measurement procedures.

6.5 Combined exposure evaluation of correlated EM sources

6.5.1 Accurate estimate of the true field vector sum

The accurate combined exposure evaluation for N EM sources emitting correlated waveforms with variable magnitude and phase relationships necessarily requires estimating the magnitude of the vector-sum of the individual fields (or their complex envelopes) as shown:

$$\left|\mathbf{e}(\mathbf{r})\right|_{rms}^2 = \left|\sum_{k=1}^{N} \mathbf{e}_k(\mathbf{r})\right|_{rms}^2 = \sum_{w=x,y,z} \left|\sum_{k=1}^{N} e_k^w(\mathbf{r})\right|_{rms}^2 = \frac{1}{2} \sum_{w=x,y,z} \left|\sum_{k=1}^{N} E_k^w(\mathbf{r})\right|_{rms}^2 . \tag{6}$$

where $\mathbf{e}_k(\mathbf{r},t) = \hat{\mathbf{x}}\, e_k^x(\mathbf{r},t) + \hat{\mathbf{y}}\, e_k^y(\mathbf{r},t) + \hat{\mathbf{z}}\, e_k^z(\mathbf{r},t), k = 1 \cdots N$.

One possible way to determine the maximum achievable exposure is by setting the sources at maximum power levels and sweeping through the possible phase combinations. For instance, the r.m.s. value of the sum of N generic time-harmonic signals modulated by a carrier with radian frequency ω_0 and magnitude, source phase, propagation delay $A_k, \phi_k, \Delta t_k, k = 1 \cdots N$, respectively, would be:

$$\left|\sum_{k=1}^{N} A_k \cos\left(\omega_0 t + \phi_k - \omega_0 \Delta t_k\right)\right|_{rms}^2 = \sum_{k=1}^{N}\sum_{h=1}^{N} \frac{A_k A_h}{2} \cos\left[\left(\phi_k - \omega_0 \Delta t_k\right) - \left(\phi_h - \omega_0 \Delta t_h\right)\right]. \quad (7)$$

Sweeping all source phases $\{\phi_1 \cdots \phi_N\}$ across their respective ranges allows capturing the maximum realized r.m.s value over the measurement domain. However, this may be very time-consuming since phase sweeps would have to be performed at every measurement point or, conversely, a complete scan of the entire set of measurement points would have to be performed for each phase combination. One advantage of this method is that it would allow using conventional scalar probes.

NOTE 1 The upper-bound for Equation (7) occurs when the arguments of all the cosine functions vanish, which happens if the source phases are chosen as $\phi_k = \omega_0 \Delta t_k, k = 1 \cdots N$. Applying this choice to each field component in fact corresponds to adopting the *conservative* approach presented in Subclause 6.5.2.3, which typically produces an overestimation of the exposure since the condition $\phi_k = \omega_0 \Delta t_k, k = 1 \cdots N$ may not be physically realizable for all three field polarisations simultaneously because, in general, each field component exhibits a different time delay.

Another approach would entail activating one source at a time to measure the magnitude and phase of the field components at every measurement point, then performing the field superposition and the aforementioned phase sweeps computationally to determine the maximum realizable r.m.s. field values at every point. In this case, measurements would require vector probes and receivers (e.g., a network analyzer in a suitable laboratory setting).

Note that additional complexity may arise when dealing with digitally modulated signals, since in this case the phase of the RF signal may be modulated by a bit stream carrying the encoded information. Therefore, accurate phase measurements may require demodulating the RF waveform. In fact, based on the results in Annex B, B.3, the field components may be written in terms of the real ($\Re$) and imaginary ($\Im$) part of the field envelope components as:

$$e_k^w(\mathbf{r},t) = \left|E_k^w(\mathbf{r},t)\right| \cos\left[\omega_0 t + \phi_k^w(\mathbf{r},t)\right], \text{ with } \phi_k^w(\mathbf{r},t) = \arctan\left[\frac{\Im\left\{E_k^w(\mathbf{r},t)\right\}}{\Re\left\{E_k^w(\mathbf{r},t)\right\}}\right], \quad (8)$$

and $w = x, y, z$. The critical requisite for reconstructing accurately the field vectors from each individual source is the accurate evaluation of the phase differences between the components of the individual fields. To this purpose, the field-component complex envelopes allowing the phase retrieval, e.g., via Equation (8), may be determined through signal correlators after suitable demodulation. Therefore, for digitally modulated signals, the accurate estimation of the total r.m.s. field may entail the use of vector probes and digital correlator receivers.

NOTE 2 Implementing this rigorous approach in experimental evaluation techniques may involve significant equipment upgrades and increased complexity in measurement procedures. For instance, *vector* sensors capable of measuring magnitude and phase of each field component, and *digital correlator* receivers, may be required.

6.5.2 Conservative combined exposure evaluation using scalar sensors

6.5.2.1 General aspects

Due to the complexity in measuring the true field vector sum (explained in 6.5.1), it is desirable to allow the use of widely-available scalar field sensors when evaluating the combined exposure from multiple correlated EM sources. In the following subclauses, two conservative approaches are illustrated which allow the use of scalar sensors, while introducing distinct levels of exposure overestimation and involving correspondingly distinct complexity in the evaluation procedure.

6.5.2.2 Combination of *SAR* or power density from correlated EM sources

A first conservative approach that would still allow retaining the advantages associated with scalar field sensors is based on the summation of the field magnitudes from the individual sources, leading to the following *SAR* and power density upper bounds (see Annex B, B.4 for the analytical derivation):

$$SAR_T(\mathbf{r}) \leq \left(\sum_{k=1}^{N} \sqrt{SAR_k(\mathbf{r})} \right)^2 , \tag{9}$$

$$S_T(\mathbf{r}) \leq \left(\sum_{k=1}^{N} \sqrt{S_k(\mathbf{r})} \right)^2 . \tag{10a}$$

NOTE 1 When frequency-dependent power density limits ($S_{\lim}(f_k)$, f_k being the mid-band frequencies of the signals $s_k(t), k = 1 \cdots N$) apply, the summation may be expressed in terms of *exposure quotients* as:

$$EQ_T(\mathbf{r}) \leq \left(\sum_{k=1}^{N} \sqrt{EQ_k(\mathbf{r})} \right)^2 = \left(\sum_{k=1}^{N} \sqrt{\frac{S_k(\mathbf{r})}{S_{\lim}(f_k)}} \right)^2 \qquad 10b)$$

Observe that for the signals to be correlated their respective bands should overlap, so typically $f_1 \approx f_2 \approx \cdots f_N$.

NOTE 2 Implicit in the derivation of Equations (9) and (10) is the assumption that the complex envelopes of the space-time fields produced by the individual sources are spatially and temporally "in-phase" everywhere, thus eliminating the need to perform relative phase measurements and to discriminate field polarisations. Therefore, commonly available isotropic scalar field probes may be readily employed to perform combined exposure evaluations according to this approach.

6.5.2.3 Combination of the magnitudes of the local field components

A second conservative approach providing *SAR* and power density distribution estimates as a function of the field components may be expressed as follows (see Annex B, B.5 for the analytical derivation):

$$SAR_T(\mathbf{r}) \leq \frac{\sigma(\mathbf{r})}{\rho(\mathbf{r})} \sum_{w=x,y,z} \left(\sum_{k=1}^{N} \left| e_k^w(\mathbf{r}) \right|_{rms} \right)^2 = \frac{\sigma(\mathbf{r})}{2\rho(\mathbf{r})} \sum_{w=x,y,z} \left(\sum_{k=1}^{N} \left| E_k^w(\mathbf{r}) \right|_{rms} \right)^2 , \tag{11}$$

$$S_T(\mathbf{r}) \leq \frac{1}{\eta_0} \sum_{w=x,y,z} \left(\sum_{k=1}^{N} \left| e_k^w(\mathbf{r}) \right|_{rms} \right)^2 = \frac{1}{2\eta_0} \sum_{w=x,y,z} \left(\sum_{k=1}^{N} \left| E_k^w(\mathbf{r}) \right|_{rms} \right)^2 . \tag{12a}$$

NOTE 1 When frequency-dependent power density limits apply, the summation may be expressed in terms of *exposure quotients* as:

$$EQ_T(\mathbf{r}) \leq \sum_{w=x,y,z} \left(\sum_{k=1}^{N} \sqrt{EQ_k^w(\mathbf{r})} \right)^2 = \sum_{w=x,y,z} \left(\sum_{k=1}^{N} \sqrt{\frac{S_k^w(\mathbf{r})}{S_{\lim}(f_k)}} \right)^2 , \text{ with } S_k^w(\mathbf{r}) = \frac{1}{\eta_0} \left| e_k^w(\mathbf{r}) \right|_{rms}^2 \tag{12b}$$

This approach introduces a lower degree of overestimation than the one in Subclause 6.5.2.2 does since it does not presume that the complex field envelopes are spatially "in-phase", as intuitively shown in Figure 4 for the two-dimensional case. The trade-off required to achieve the smaller overestimation is that all field-component magnitudes be measured independently and that the local reference frame at each field-point be kept the same for all sources measured in succession so the homonymous magnitudes may be added properly.

NOTE 2 This approach may be readily implemented in controlled laboratory setups such as those employed for *SAR* measurements according to the IEC 62209-1 and IEC 62209-2 standards, where the isotropic E-field probes incorporating miniature orthogonal diode-detector sensors are scanned using robots in a very repeatable fashion.

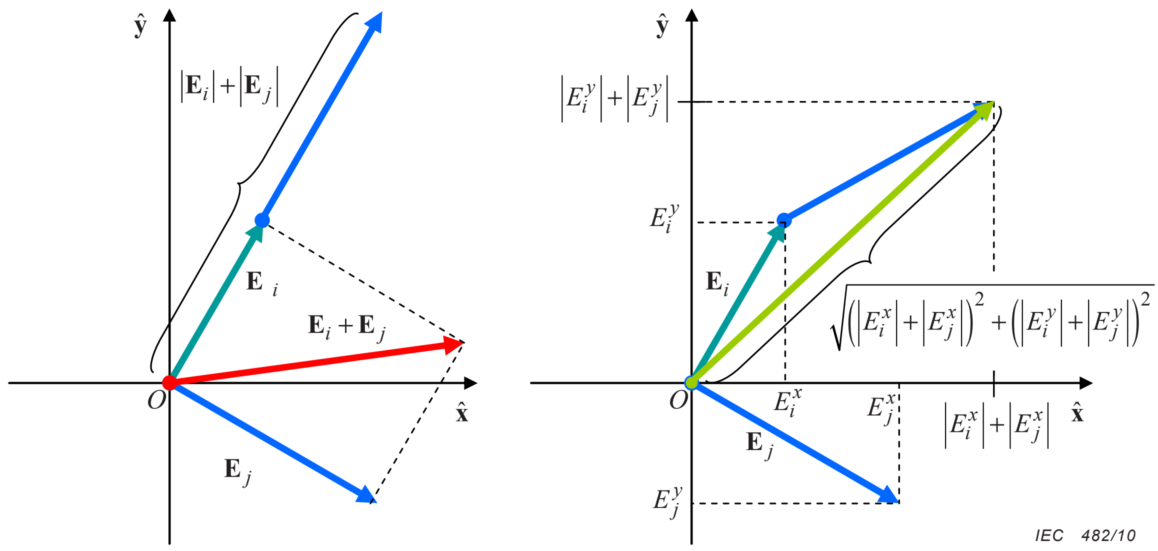

Figure 4 – Different approaches yielding distinct upper-bounds of the field vector-sum

a) the r.m.s. complex field envelopes are assumed “in phase” temporally and spatially, as per Equations (9) and (10), yielding a conservative field magnitude estimate;

b) the r.m.s. field-component envelopes are assumed “in phase” temporally, as per Equations (11) and (12), yielding a smaller overestimate of the true field vector-sum (red arrow).

Annex A
(informative)

Frequency allocations for some common wireless services

Table A.1 lists a representative set, with no pretence of completeness, of existing and upcoming wireless communications services worldwide, providing their respective frequency allocations and absolute (kHz) or fractional (%) channels bandwidths. The corresponding maximum contiguous (up-link or down-link) bandwidths are also reported since emissions from node-centric devices may require measurements over such entire bands. The large majority of listed wireless communication systems feature fractional channel bandwidths well below 10 %, the notable exceptions being TV and FM radio services. The maximum contiguous broadcast (down-link) bandwidths for such services may also exceed significantly the 10 % threshold, particularly for TV, thus applicable standards should provide guidance on methods and instrumentation required to characterize the exposure due to field emission from transmitters, e.g. TV repeaters, emitting composite waveforms comprising a large number of channels occupying vast spectrum swaths where field exposure limits may vary significantly.[5]

Table A.1 – Frequency allocations and bandwidths for common wireless technologies

Service	Frequency band [MHz]		Channel bandwidth		Maximum contiguous up/down-link bandwidth	
	UP-LINK	DOWN-LINK	kHz	%	MHz	%
NFC	13,56		≤ 14	≤ 0,1 %	0,014	0,1 %
TV	47 ~ 68		≤ 6 000	≤ 12,8 %	21	>> 10 %
	48 ~ 100				52	
	52 ~ 88				36	
	90 ~ 108				18	
	170 ~ 230				60	
	470 ~ 692				222	
	470 ~ 770				300	
	470 ~ 870				400	
	526 ~ 820				294	
FM radio	65 ~ 74		≤ 200	≤ 0,31 %	9	≤ 13 %
	76 ~ 90				14	≤ 17 %
	87,5 ~ 108				20,5	≤ 21 %
US Public Safety	136 ~ 148 / 148 ~ 162 / 162 ~ 174 406 ~ 420 / 450 ~ 470 / 470 ~ 512 806 ~ 824 / 851 ~ 869		≤ 25	≤ 0,018 %	≤ 42	≤ 9,0 %
TETRA	380 ~ 390	390 ~ 400	25	≤ 0,007 %	≤ 10	≤ 2,6 %
	410 ~ 420	420 ~ 430				
	806 ~ 811	851 ~ 856			5	≤ 0,6 %
AMPS/NAMPS	824 ~ 849	869 ~ 894	≤ 30	≤ 0,004 %	25	≤ 3,0 %

5 For instance, exposure from fields produced by node-centric devices emitting wideband composite waveforms may be evaluated by performing frequency-selective measurements over contiguous bands covering the whole transmit band, and computing the sum of the *exposure quotients* per Equation (5b).

Service	Frequency band [MHz]		Channel bandwidth		Maximum contiguous up/down-link bandwidth	
	UP-LINK	DOWN-LINK	kHz	%	MHz	%
D-AMPS (TDMA)	824 ~ 849	869 ~ 894	30	≤ 0,004 %	25	≤ 3,0 %
GSM (GSM, GSM-R, E-GSM)	824 ~ 849	869 ~ 894	200	≤ 0,024 %	25	≤ 3,0 %
	876 ~ 915	921 ~ 960			39	≤ 4,3 %
	1 710 ~ 1 785	1 805 ~ 1 880			75	≤ 4,3 %
	1 850 ~ 1 910	1 930 ~ 1 990			60	≤ 3,2 %
TACS 600/1000 E-TACS	872 ~ 915	917 ~ 960	25	≤ 0,003 %	43	≤ 4,8 %
JTACS	887 ~ 925	832 ~ 870	25	≤ 0,003 %	38	≤ 4,6 %
CDMA (IS-95)	824 ~ 849	869 ~ 894	1 320	≤ 0,161 %	25	≤ 3,0 %
	1 750 ~ 1 780	1 840 ~ 1 870			30	≤ 1,7 %
CDMA 2000 (Class 0, 3, 6)	824 ~ 924	832 ~ 869	1 250	≤ 0,152 %	38	≤ 4,6 %
	1 920 ~ 1 980	2 110 ~ 2 170			60	≤ 3,2 %
DECT	1880 ~ 1980 2010 ~ 2025 2400 ~ 2483,5		1 728	≤ 0,092 %	100	≤ 5,2 %
PDC	940 ~ 958	810 ~ 828	50	≤ 0,006 %	18	≤ 2,2 %
	893 ~ 895	838 ~ 840			2	≤ 0,24 %
	925 ~ 940	870 ~ 885			15	≤ 1,7 %
	1 429 ~ 1 453	1 477 ~ 1 501			24	≤ 1,7 %
PHS	1 884 ~ 1 920		300	≤ 0,016 %	36	1,9 %
XGP (next-G PHS)	2 545 ~ 2 625		10 000	0,39 %	80	3,1 %
UMTS (W-CDMA) Band I, VI, IX	830 ~ 840	875 ~ 885	5 000	≤ 0,603 %	10	≤ 1,2 %
	1 750 ~ 1 785	1 845 ~ 1 880			35	≤ 2,0 %
	1 920 ~ 1 980	2 110 ~ 2 170			60	≤ 3,2 %
Bluetooth	2 400 ~ 2 483,5		1 000	≤0,042 %	83,5	≤ 3,4 %

Service	Frequency band [MHz]		Channel bandwidth		Maximum contiguous up/down-link bandwidth	
	UP-LINK	DOWN-LINK	kHz	%	MHz	%
WiMAX/LTE Band 1-14, 17	698 ~ 716	728 ~ 746	≤ 20 000	< 2,9 %	18	≤ 2,5 %
	704 ~ 716	734 ~ 746			12	≤ 1,7 %
	777 ~ 787	746 ~ 756			10	≤ 1,3 %
	788 ~ 798	758 ~ 768			10	≤ 1,3 %
	824 ~ 849	869 ~ 894			25	≤ 3,0 %
	830 ~ 840	875 ~ 885			10	≤ 1,2 %
	880 ~ 915	925 ~ 960			35	≤ 3,9 %
	1 427-1 453	1 475 ~ 1 501			26	≤ 1,8 %
	1 710 ~ 1 755	2 110 ~ 2 155			45	≤ 2,6 %
	1 710 ~ 1 770	2 110 ~ 2 170			60	≤ 3,4 %
	1 710 ~ 1 785	1 805 ~ 1 880			75	≤ 4,3 %
	1 749 ~ 1 785	1 844 ~ 1 880			36	≤ 2,0 %
	1 850 ~ 1 910	1 930 ~ 1 990			60	≤ 3,2 %
	1 920 ~ 1 980	2 110 ~ 2 170			60	≤ 3,1 %
	2 500 ~ 2 570	2 620 ~ 2 690			70	≤ 2,8 %
	3 400 ~ 3 600				200	≤ 5,7 %
	5 250 ~ 5 350				100	≤ 1,9 %
	5 470 ~ 5 725				255	≤ 4,6 %
	5 725 ~ 5 850				125	≤ 2,2 %
WiMAX (Wi-Bro)	2 300 ~ 2 358,5		9 000	≤ 0,392 %	58,5	≤ 2,5 %
Wi-Fi	2 400 ~ 2 483,5		26 000	≤ 1,09 %	83,5	≤ 3,4 %
	5 150 ~ 5 250		70 000	≤ 1,36 %	100	≤ 1,9 %
	5 250 ~ 5 350				100	≤ 1,9 %
	5 470 ~ 5 750				280	≤ 5,0 %
	5 750 ~ 5 850				100	≤ 1,7 %

Annex B
(informative)

Supporting analytical details

B.1 Complex envelope of the EM field

Particularly for the case of waveforms modulated by a carrier frequency f_0, it is convenient to define analogues to the electromagnetic field phasors. For linear, time invariant media, the electric field produced at time t at a point $\mathbf{r}$ in space due to a current distribution $\mathbf{j}$ excited on a domain V is given by the integral between the current and a suitable dyadic function $\underline{\mathbf{g}}$ representing the electric field space-time impulse response in the field domain:

$$\mathbf{e}(\mathbf{r},t)=\iiint_V \int_{-\infty}^{+\infty} \underline{\mathbf{g}}(\mathbf{r}\,|\,\mathbf{r}',t-\tau)\cdot\mathbf{j}(\mathbf{r}',\tau)\,d\tau\,dV'. \tag{B.1}$$

Without loss of generality, assuming the current source domain is a point ($V\equiv\{\mathbf{r}_0\}$), the source-point current can be readily expressed as a function of the signal waveform $s(t)$ as:

$$\mathbf{j}(\mathbf{r}',t)=\hat{\mathbf{p}}_0\,(\ell I_0)\,\delta(\mathbf{r}'-\mathbf{r}_0)\,s(t), \tag{B.2}$$

where $\hat{\mathbf{p}}_0$ is a unit vector indicating the source orientation, δ is the Dirac-impulse function, I_0 is a nominal source-point current and ℓ the source equivalent length (formally introduced to reconcile dimensions). Introducing the real-valued vector $\mathbf{g}_0(\mathbf{r},t)=(\ell I_0)\underline{\mathbf{g}}(\mathbf{r}\,|\,\mathbf{r}_0,t)\cdot\hat{\mathbf{p}}_0$, the field may be expressed as a time-domain convolution (symbol $*$):

$$\mathbf{e}(\mathbf{r},t)=\mathbf{g}_0(\mathbf{r},t)*s(t)=\int_{-\infty}^{+\infty}\mathbf{g}_0(\mathbf{r},\tau)\,s(t-\tau)\,d\tau. \tag{B.3}$$

Since $s(t)$ is a real-valued function, it can be conveniently expressed through its complex envelope $\overline{s}(t)$, which contains the transmitted information suitably encoded, as follows: [6]

$$s(t)=\Re\left\{\overline{s}(t)\,e^{j\omega_0 t}\right\}, \tag{B.4}$$

with $\omega_0=2\pi f_0$ and $\Re\{\cdot\}$ the real-part operator, thus yielding:

$$\begin{aligned}\mathbf{e}(\mathbf{r},t)&=\mathbf{g}_0(\mathbf{r},t)*s(t)=\int_{-\infty}^{+\infty}\mathbf{g}_0(\mathbf{r},\tau)\,\Re\left\{\overline{s}(t-\tau)\,e^{j\omega_0(t-\tau)}\right\}d\tau\\&=\Re\left\{\left[\int_{-\infty}^{+\infty}\mathbf{g}_0(\mathbf{r},\tau)\,e^{-j\omega_0\tau}\,\overline{s}(t-\tau)\,d\tau\right]e^{j\omega_0 t}\right\}=\Re\left\{\mathbf{E}(\mathbf{r},t)\,e^{j\omega_0 t}\right\},\end{aligned} \tag{B.5}$$

6 This analysis makes use of signal theory concepts, e.g., see A. Papoulis, *Signal Analysis*, McGraw-Hill (1977).

having defined the complex envelope of the electric field (analogue of the phasor for time-harmonic signals) as:

$$\mathbf{E}(\mathbf{r},t)=\left[\mathbf{g}_0(\mathbf{r},t)e^{-j\omega_0 t}\right]*\overline{s}(t). \quad \text{(B.6)}$$

Observe that if $\mathbf{G}_0(\mathbf{r},t)$ is the complex envelope of $\mathbf{g}_0(\mathbf{r},t)$ then $\mathbf{E}(\mathbf{r},t)=\frac{1}{2}\mathbf{G}_0(\mathbf{r},t)*\overline{s}(t)$.

B.2 Correlation between fields emitted by two narrowband EM sources

B.2.1 Dependence of the field correlation on the signal correlation

The time-domain correlation (symbol $\otimes$) between two fields $\mathbf{e}_i(\mathbf{r},t),\mathbf{e}_j(\mathbf{r},t)$ is defined as:

$$\xi_{ij}(\mathbf{r},t)=\left(\mathbf{e}_i\otimes\mathbf{e}_j\right)(\mathbf{r},t)=\lim_{T\to\infty}\frac{1}{2T}\int_{-T}^{+T}\mathbf{e}_i(\mathbf{r},\tau)^{+}\cdot\mathbf{e}_j(\mathbf{r},t+\tau)\,d\tau. \quad \text{(B.7)}$$

NOTE This definition presumes that the fields may be observed over an infinite time, which is useful to establish a convenient analytical framework for the demonstrations that follow. However, in reality field measurements are carried out over short time intervals. Therefore, the above definition must be put in proper context. In particular, it should be remarked that the considerations regarding signal and field correlations, when applied to measurements, are valid provided measurements are carried out over a time interval that allows capturing the essential signal characteristics, e.g., average power and signal correlation. For instance, in the case of CDMA waveform encoded with Wash codes and pseudo-random noise (PN) sequences having strong orthogonality properties, the measurements need to be carried out over many signal frames since each frame includes a complete PN sequence. For instance, in the case of the CDMA IS-95 standard, each downlink signal is spread with a Walsh code of length 64 and a PN sequence of length 2^{15}, yielding a frame of about 26,7 ms. Therefore, a measurement lasting 1 s would capture more than 37 full PN sequence repetitions, enough to characterize signal and field correlations with sufficient accuracy. This aspect is further addressed in Annex B, B.3.

The fields are excited by respective point sources placed at the locations identified by the vectors $\mathbf{r}_i,\mathbf{r}_j$, featuring point-source currents $\mathbf{j}_k(\mathbf{r},t)=\hat{\mathbf{p}}_k(\ell I_k)\delta(\mathbf{r}-\mathbf{r}_k)s_k(t), k=i,j$.

Upon defining the real-valued vectors $\mathbf{g}_k(\mathbf{r},t)=(\ell I_k)\underline{\mathbf{g}}(\mathbf{r}\,|\,\mathbf{r}_k,t)\cdot\hat{\mathbf{p}}_k, k=i,j$, the fields can be written similarly to Equation (B.3) as $\mathbf{e}_k(\mathbf{r},t)=\mathbf{g}_k(\mathbf{r},t)*s_k(t)$. After some algebra, the sought dependence is established as follows:

$$\xi_{ij}(\mathbf{r},t)=\left[\mathbf{g}_i(\mathbf{r},t)*s_i(t)\right]\otimes\left[\mathbf{g}_j(\mathbf{r},t)*s_j(t)\right]=\left(\mathbf{g}_i\otimes\mathbf{g}_j\right)(\mathbf{r},t)*\left(s_i\otimes s_j\right)(t). \quad \text{(B.8)}$$

Therefore, a sufficient condition for the field correlation to vanish identically is that the signals be uncorrelated. The geometrical field orthogonality would make the field correlation vanish as well. While the former condition only depends on the signal characteristics, and therefore it would produce uncorrelated fields everywhere, the latter depends on the field domain geometry and may only occur under special circumstances, e.g., propagation of orthogonally polarized plane-waves in free space, and possibly only at select points. Therefore, the only considerations that have practical relevance in the context of this Technical Report are those regarding the signal correlation function $(s_i\otimes s_j)(t)$. Hence the signal characteristics influencing the signal correlation function are analysed in detail in the following subclauses.

B.2.2 Signals with overlapping bands

The correlation between two real-valued signals $s_k(t), k=i,j$ occupying the overlapping frequency bands $B_k\equiv\{f\,|\,f_k^{\min}<|f|<f_k^{\max}\}$ with $B_i\cap B_j\neq\varnothing$, depends on the correlation

between the respective complex envelopes $\overline{s}_k(t), k = i, j$. In fact, the relationship between the signals and their complex envelopes is:

$$s_k(t) = \Re\left\{\overline{s}_k(t) e^{j\omega_0 t}\right\} \quad , k = i, j, \tag{B.9}$$

with $\omega_0 = 2\pi f_0$ where f_0 is the frequency chosen to define said complex envelopes. Likewise, the correlation integral between the signals may be expressed through its complex envelope $\overline{\rho}_{ij}(t)$, relative to the same frequency f_0, as follows:

$$\rho_{ij}(t) = \left(s_i \otimes s_j\right)(t) = \lim_{T\to\infty} \frac{1}{2T} \int_{-T}^{+T} s_i(\tau)^+ s_j(t+\tau)\, d\tau = \Re\left\{\overline{\rho}_{ij}(t) e^{j\omega_0 t}\right\} \tag{B.10}$$

Due to known properties of the convolution product between two real-valued functions (i.e., if $z(t) = x(t) * y(t)$ then $\overline{z}(t) = \frac{1}{2}\overline{x}(t) * \overline{y}(t)$, and $(x \otimes y)(t) = x(-t) * y(t)$), the signal correlation may be expressed as:

$$\rho_{ij}(t) = \Re\left\{\overline{\rho}_{ij}(t) e^{j\omega_0 t}\right\} = \frac{1}{2}\Re\left\{\left(\overline{s}_i \otimes \overline{s}_j\right)(t) e^{j\omega_0 t}\right\} \tag{B.11}$$

Therefore, two signals are uncorrelated if their complex envelopes, relative to the same frequency f_0, are uncorrelated, i.e., $(\overline{s}_i \otimes \overline{s}_j)(t) \equiv 0$. For signals featuring partially or totally overlapped bands, fulfilling this condition may depend on the respective communication protocols, e.g., the way information is encoded.

Observe that the above conclusions hold in general, regardless of whether the signals are narrowband or wideband, and whether they are carrier-modulated or at baseband.

NOTE Choosing $f_0 \in B_i \cap B_j$ may be convenient so the complex envelopes are at base band, but it is not strictly necessary. For signals sharing the same band $B \equiv \{f \mid f^{\min} < |f| < f^{\max}\}$, a typical choice is $f_0 = (f^{\min} + f^{\max})/2$.

B.2.3 Signals with disjoint bands

Two signals $s_k(t), k = i, j$ occupying disjoint frequency bands ($B_i \cap B_j \equiv \varnothing$) may be rewritten:

$$s_k(t) = h_k(t) * s_k(t) \quad , k = i, j \tag{B.12)}$$

where the functions $h_k(t), k = i, j$ are the impulse responses corresponding to ideal band-pass filters associated with each signal band,[7] having Fourier transforms:

$$H_k(f) = \begin{cases} 1, & f \in B_k \\ 0, & f \notin B_k \end{cases} \quad , k = i, j \tag{B.13)}$$

After some algebra, the signal correlation becomes:

[7] These ideal filters are introduced since their impulse responses are energy limited thus they admit Fourier transforms, while the signals themselves may not be energy limited thus they may not admit Fourier transforms.

$$\rho_{ij}(t) = \left[h_i(t) * s_i(t)\right] \otimes \left[h_j(t) * s_j(t)\right] = \left(h_i \otimes h_j\right)(t) * \left(s_i \otimes s_j\right)(t). \qquad \text{(B.14)}$$

The Fourier transform of the correlation function involving the filter impulse responses $h_k(t), k = i, j$ is given by:

$$\mathcal{F}\left\{\left(h_i \otimes h_j\right)(t)\right\} = H_i(f)^{+} H_j(f) \equiv 0 \qquad \text{(B.15)}$$

so it vanishes identically since the transforms $H_k(f), k = i, j$ are non-zero in separate, non-overlapping bands. Consequently $(h_i \otimes h_j)(t) \equiv 0$ and therefore, from Equation (B.14) it follows that $\rho_{ij}(t) = (s_i \otimes s_j)(t) \equiv 0$, hence $\xi_{ij}(\mathbf{r},t) = (\mathbf{e}_i \otimes \mathbf{e}_j)(\mathbf{r},t) \equiv 0$ due to Equation (B.8).

NOTE This result allows concluding that signals occupying disjoint bands always produce uncorrelated fields.

B.3 Expressions for the r.m.s. electric field

Dosimetric (*SAR*) and densitometric (power density) exposure metrics may be expressed in terms of the local r.m.s. electric field, defined as follows:

$$\left|\mathbf{e}(\mathbf{r})\right|_{rms} = \sqrt{\lim_{T\to\infty}\frac{1}{2T}\int_{-T}^{+T}\left|\mathbf{e}(\mathbf{r},\tau)\right|^2 d\tau} = \sqrt{\lim_{T\to\infty}\frac{1}{2T}\int_{-T}^{+T}\mathbf{e}(\mathbf{r},\tau)^{+}\cdot\mathbf{e}(\mathbf{r},\tau)\,d\tau}\,. \qquad \text{(B.16a)}$$

NOTE As remarked in Annex B, B.2.1, the infinite extension of the integral bounds in the above definition is useful to establish a convenient analytical framework, but it should be put in proper context when applied to field measurements. Specifically, if a measurement interval ΔT is deemed sufficient to capture the essential signal characteristics, e.g., average power and correlation, then the r.m.s. field definition can be adapted as follows:

$$\left|\mathbf{e}(\mathbf{r},t)\right|_{rms} = \sqrt{\frac{1}{\Delta T}\int_{t-\Delta T/2}^{t+\Delta T/2}\left|\mathbf{e}(\mathbf{r},\tau)\right|^2 d\tau} \qquad \text{(B.16b)}$$

Observe that, according to this adapted definition, the r.m.s. field is a function of time since the evaluation is performed over the sliding time window ΔT. This is in fact what is normally done when monitoring ambient fields.

From the definition pf r.m.s. electric field [Equation (B.16a)] and Equation (B.7), it is readily seen that the r.m.s. field may be expressed in terms of the field autocorrelation at time $t = 0$:

$$\left|\mathbf{e}(\mathbf{r})\right|_{rms} = \sqrt{(\mathbf{e}\otimes\mathbf{e})(\mathbf{r},t)}\Big|_{t=0} = \sqrt{\langle\mathbf{e},\mathbf{e}\rangle(\mathbf{r})} \qquad \text{(B.17)}$$

the last member of this equation featuring an inner product, since the correlation integral at time $t = 0$ exhibits the properties of a suitably defined inner product:

$$\langle\mathbf{u},\mathbf{v}\rangle = \lim_{T\to\infty}\frac{1}{2T}\int_{-T}^{+T}\mathbf{u}(\tau)^{+}\cdot\mathbf{v}(\tau)\,d\tau \qquad \text{(B.18)}$$

with $\mathbf{u},\mathbf{v}$ being time-dependent complex vectors. The r.m.s. field can be readily linked to its complex envelope as well as the r.m.s. value of the latter by applying Equation (B.11) to the autocorrelation integrals of its orthogonal components $e_w(\mathbf{r},t), w = x, y, z$, yielding:

$$\begin{aligned}\left|\mathbf{e}(\mathbf{r})\right|_{rms}^{2} &= (\mathbf{e}\otimes\mathbf{e})(\mathbf{r},0) = \sum_{w=x,y,z}(e_w\otimes e_w)(\mathbf{r},0) = \sum_{w=x,y,z}\frac{1}{2}(E_w\otimes E_w)(\mathbf{r},0) \\ &= \frac{1}{2}(\mathbf{E}\otimes\mathbf{E})(\mathbf{r},0) = \frac{1}{2}\langle\mathbf{E},\mathbf{E}\rangle(\mathbf{r}) = \frac{1}{2}\left|\mathbf{E}(\mathbf{r})\right|_{rms}^{2} \quad ,\end{aligned} \tag{B.19}$$

where $E_w(\mathbf{r},t), w=x,y,z$ are the complex envelopes of the field components. Based on the above considerations, *SAR* and power density assume any one of the following expressions:

$$SAR(\mathbf{r}) = \frac{\sigma(\mathbf{r})}{\rho(\mathbf{r})}\left|\mathbf{e}(\mathbf{r})\right|_{rms}^{2} = \frac{\sigma(\mathbf{r})}{\rho(\mathbf{r})}\langle\mathbf{e},\mathbf{e}\rangle(\mathbf{r}) = \frac{\sigma(\mathbf{r})}{2\rho(\mathbf{r})}\langle\mathbf{E},\mathbf{E}\rangle(\mathbf{r}) = \frac{\sigma(\mathbf{r})}{2\rho(\mathbf{r})}\left|\mathbf{E}(\mathbf{r})\right|_{rms}^{2} \tag{B.20}$$

$$S(\mathbf{r}) = \frac{1}{\eta_0}\left|\mathbf{e}(\mathbf{r})\right|_{rms}^{2} = \frac{1}{\eta_0}\langle\mathbf{e},\mathbf{e}\rangle(\mathbf{r}) = \frac{1}{2\eta_0}\langle\mathbf{E},\mathbf{E}\rangle(\mathbf{r}) = \frac{1}{2\eta_0}\left|\mathbf{E}(\mathbf{r})\right|_{rms}^{2} \tag{B.21}$$

These equations show explicitly that the characteristics of *SAR* and power density may be derived indifferently from the space-time fields or from their complex envelopes.

B.4 Proof of Equations (4) and (5) [6.4]

When two EM sources emit uncorrelated signal waveforms $s_i(t), s_j(t)$ $[(s_i\otimes s_j)(t)\equiv 0]$, with correspondingly uncorrelated field distributions $\mathbf{e}_i(\mathbf{r},t),\mathbf{e}_j(\mathbf{r},t)$ $[(\mathbf{e}_i\otimes\mathbf{e}_j)(\mathbf{r},t)\equiv 0]$, the r.m.s. value of the total field $\mathbf{e}(\mathbf{r},t)=\mathbf{e}_i(\mathbf{r},t)+\mathbf{e}_j(\mathbf{r},t)$ is:[8]

$$\begin{aligned}\left|\mathbf{e}(\mathbf{r})\right|_{rms}^{2} &= \langle\mathbf{e},\mathbf{e}\rangle = \langle\mathbf{e}_i+\mathbf{e}_j,\mathbf{e}_i+\mathbf{e}_j\rangle = \langle\mathbf{e}_i,\mathbf{e}_i\rangle+\langle\mathbf{e}_i,\mathbf{e}_j\rangle+\langle\mathbf{e}_j,\mathbf{e}_i\rangle+\langle\mathbf{e}_j,\mathbf{e}_j\rangle \\ &= \langle\mathbf{e}_i,\mathbf{e}_i\rangle+\langle\mathbf{e}_j,\mathbf{e}_j\rangle = \left|\mathbf{e}_i(\mathbf{r})\right|_{rms}^{2}+\left|\mathbf{e}_j(\mathbf{r})\right|_{rms}^{2} \quad ,\end{aligned} \tag{B.22}$$

since by definition $\langle\mathbf{e}_i,\mathbf{e}_j\rangle=(\mathbf{e}_i\otimes\mathbf{e}_j)(\mathbf{r},0)=0$ if $i\neq j$. This expression may be readily generalized to the case of three or more uncorrelated EM sources, showing that each source contributes to the combined exposure metrics (*SAR* and *S*) independently.

NOTE The above proof, as well as those that follow, can also be carried out using the complex field envelope and the corresponding inner product. In this case, the inner products are generally complex functions.

B.5 Proof of Equations (9) and (10) [6.5.2.2]

Using the following inequalities:

$$\Re\{\zeta\}\leq|\zeta| \tag{B.23}$$

$$\left|\langle\mathbf{u},\mathbf{v}\rangle\right|\leq|\mathbf{u}||\mathbf{v}| \tag{B.24}$$

8 For notational simplicity, the inner product functional dependence $(\mathbf{r})$ is dropped, yet implied, in the following.

where ζ is an arbitrary complex variable, and $\mathbf{u},\mathbf{v}$ are arbitrary complex vectors, it is readily seen that the following inequality holds:

$$\begin{aligned}
\left|\mathbf{e}(\mathbf{r})\right|_{rms}^{2} &= \langle \mathbf{e},\mathbf{e}\rangle = \langle \mathbf{e}_i+\mathbf{e}_j,\mathbf{e}_i+\mathbf{e}_j\rangle = \langle \mathbf{e}_i,\mathbf{e}_i\rangle + \langle \mathbf{e}_i,\mathbf{e}_j\rangle + \langle \mathbf{e}_j,\mathbf{e}_i\rangle + \langle \mathbf{e}_j,\mathbf{e}_j\rangle \\
&= \langle \mathbf{e}_i,\mathbf{e}_i\rangle + \langle \mathbf{e}_i,\mathbf{e}_j\rangle + \langle \mathbf{e}_i,\mathbf{e}_j\rangle^{+} + \langle \mathbf{e}_j,\mathbf{e}_j\rangle \\
&= \langle \mathbf{e}_i,\mathbf{e}_i\rangle + 2\Re\left\{\langle \mathbf{e}_i,\mathbf{e}_j\rangle\right\} + \langle \mathbf{e}_j,\mathbf{e}_j\rangle \\
&\le \langle \mathbf{e}_i,\mathbf{e}_i\rangle + 2\left|\langle \mathbf{e}_i,\mathbf{e}_j\rangle\right| + \langle \mathbf{e}_j,\mathbf{e}_j\rangle \qquad \text{(B.25)} \\
&\le \langle \mathbf{e}_i,\mathbf{e}_i\rangle + 2\sqrt{\left|\langle \mathbf{e}_i,\mathbf{e}_i\rangle\right|}\sqrt{\left|\langle \mathbf{e}_j,\mathbf{e}_j\rangle\right|} + \langle \mathbf{e}_j,\mathbf{e}_j\rangle \\
&\le \left|\mathbf{e}_i(\mathbf{r})\right|_{rms}^{2} + 2\left|\mathbf{e}_i(\mathbf{r})\right|_{rms}\left|\mathbf{e}_j(\mathbf{r})\right|_{rms} + \left|\mathbf{e}_j(\mathbf{r})\right|_{rms}^{2} \\
&= \left(\left|\mathbf{e}_i(\mathbf{r})\right|_{rms} + \left|\mathbf{e}_j(\mathbf{r})\right|_{rms}\right)^{2},
\end{aligned}$$

having employed the inner product commutative property ($\langle \mathbf{u},\mathbf{v}\rangle = \langle \mathbf{v},\mathbf{u}\rangle^{+}$). A geometrical interpretation of Equation (B.25) is provided in Figure B.1, which allows concluding that the inequality may be readily extended to an arbitrary number of vectors, thus an arbitrary number of EM sources operating simultaneously.

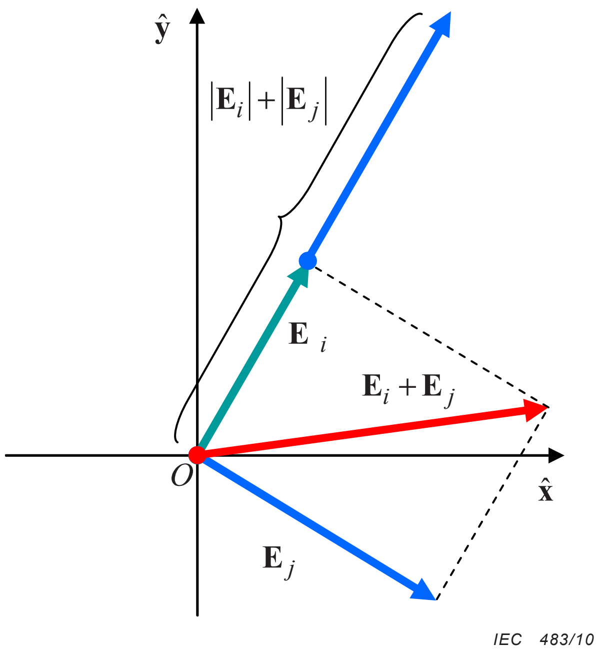

Figure B.1 – Vectorial interpretation of inequality (B25), yielding an upper-bound of the true field vector-sum (red arrow)

B.6 Proof of Equations (11) and (12) [6.5.2.3]

Expanding the individual (space-time or complex envelope) fields in terms of their respective orthogonal components (in space-time: $\mathbf{e}_k(\mathbf{r},t) = \hat{\mathbf{x}}\, e_k^x(\mathbf{r},t) + \hat{\mathbf{y}}\, e_k^y(\mathbf{r},t) + \hat{\mathbf{z}}\, e_k^z(\mathbf{r},t)$, $k = i, j$) and using the following inequality:

$$\left|\xi+\zeta\right| \le \left|\xi\right| + \left|\zeta\right| \tag{B.26}$$

where ξ, ζ are arbitrary complex variables, it is readily seen that the following inequality holds:

$$\begin{aligned}
&\left|\mathbf{e}(\mathbf{r})\right|_{rms}^{2} = \langle \mathbf{e},\mathbf{e} \rangle = \langle \mathbf{e}_i + \mathbf{e}_j, \mathbf{e}_i + \mathbf{e}_j \rangle \\
&= \langle e_i^x + e_j^x, e_i^x + e_j^x \rangle + \langle e_i^y + e_j^y, e_i^y + e_j^y \rangle + \langle e_i^z + e_j^z, e_i^z + e_j^z \rangle \\
&= \left|e_i^x(\mathbf{r}) + e_j^x(\mathbf{r})\right|_{rms}^2 + \left|e_i^y(\mathbf{r}) + e_j^y(\mathbf{r})\right|_{rms}^2 + \left|e_i^z(\mathbf{r}) + e_j^z(\mathbf{r})\right|_{rms}^2 \\
&\le \left(\left|e_i^x(\mathbf{r})\right|_{rms} + \left|e_j^x(\mathbf{r})\right|_{rms}\right)^2 + \left(\left|e_i^y(\mathbf{r})\right|_{rms} + \left|e_j^y(\mathbf{r})\right|_{rms}\right)^2 + \left(\left|e_i^z(\mathbf{r})\right|_{rms} + \left|e_j^z(\mathbf{r})\right|_{rms}\right)^2.
\end{aligned} \tag{B.27}$$

Since Equation (B.26) can be extended to an arbitrary number of complex variables, Equation (B.27) may also be extended to an arbitrary number of vectors, thus an arbitrary number of EM sources operating simultaneously.

Annex C
(informative)

Examples of combined exposure evaluations

C.1 Overview

Several examples are presented to illustrate the practical application of the principles established in this Technical Report to evaluate the combined exposure from multiple EM sources. These examples address cases that are frequently encountered when dealing with wireless communication infrastructure or terminals.

C.2 Uncorrelated sources

One of the most common cases of exposure from multiple EM sources occurs when a mobile terminal is simultaneously engaged in transmitting over multiple air-interfaces. For instance, a mobile phone may be supporting a voice call over GSM while communicating with the user's earpiece over Bluetooth. Many other similar cases are encountered in practice; see for instance the mobile phone antenna arrangement detailed in Figure C.1.

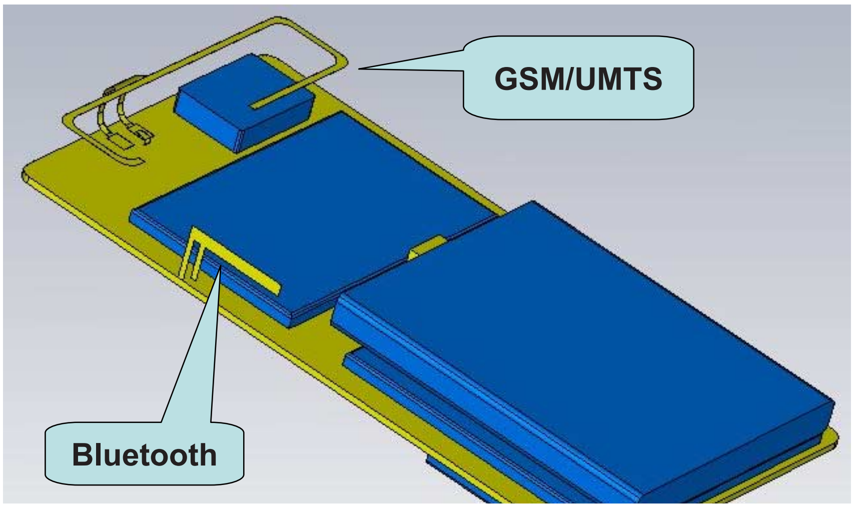

IEC 484/10

Figure C.1 – CAD model of the antenna system for a mobile phone, including a GSM/UMTS antenna and a Bluetooth antenna

Another common case involves base-station antenna sites hosting infrastructure equipment belonging to multiple network operators, which may operate in different bands (e.g., GSM at 900 MHz and UMTS at 2 100 MHz) and over distinct air-interface (e.g., GSM and CDMA). Accordingly, the next subclauses address an example of each of these two cases.

C.2.1 Combined *SAR* for a mobile phone operating in GSM and Wi-Fi

This example addresses two co-located single-channel transmitters embedded in a user-centric wireless communication device.

A multi-mode mobile phone featuring Wi-Fi connection allows the user to simultaneously engage in GSM (~1 800 MHz) voice and Wi-Fi (~2,45 GHz) data transmissions. Since GSM and Wi-Fi operate in disjoint frequency bands, the two signals are uncorrelated (see Annex B, B.2.3) so the respective *SAR* distributions may be added, as qualitatively shown in Figure C.2.

More specifically, suppose the *SAR* is measured over a set of points $R \equiv \{\mathbf{r}_n \mid n = 1, \cdots, N\}$ in a suitable head or body phantom filled with tissue-equivalent simulant (e.g., as recommended in IEC 62209-1 or IEC 62209-2). The individual *SAR* data sets for each transmit modes are determined by measuring the *SAR* over the domain R with only one mode active at a time. Therefore, when using scalar probes, there need to be at least as many measurements as the number of transmit modes. In the example at hand, the *SAR* data sets are:

GSM: $SAR_{\text{GSM}}(R) \equiv \{SAR_{\text{GSM}}(\mathbf{r}_n) \mid \mathbf{r}_n \in R\}$

Wi-Fi: $SAR_{\text{Wi-Fi}}(R) \equiv \{SAR_{\text{Wi-Fi}}(\mathbf{r}_n) \mid \mathbf{r}_n \in R\}$

According to Equation (4), the combined *SAR* distribution is then computed as the sum of the individual ones:

GSM+Wi-Fi: $SAR_{\text{GSM+Wi-Fi}}(R) \equiv \{SAR_{\text{GSM}}(\mathbf{r}_n) + SAR_{\text{Wi-Fi}}(\mathbf{r}_n) \mid \mathbf{r}_n \in R\}$

After the combined *SAR* data set is determined, the conventional operations leading to the 1-g or 10-g peak *SAR* (according to IEC 62209-1) may be performed.[9]

NOTE This approach may be very time consuming if the individual *SAR* distributions are sampled over a large volume. For this reason, the IEC 62209-2 standard recommends several alternative techniques to shorten test times significantly, which may introduce some degree of overestimation to achieve a better *SAR* testing efficiency.

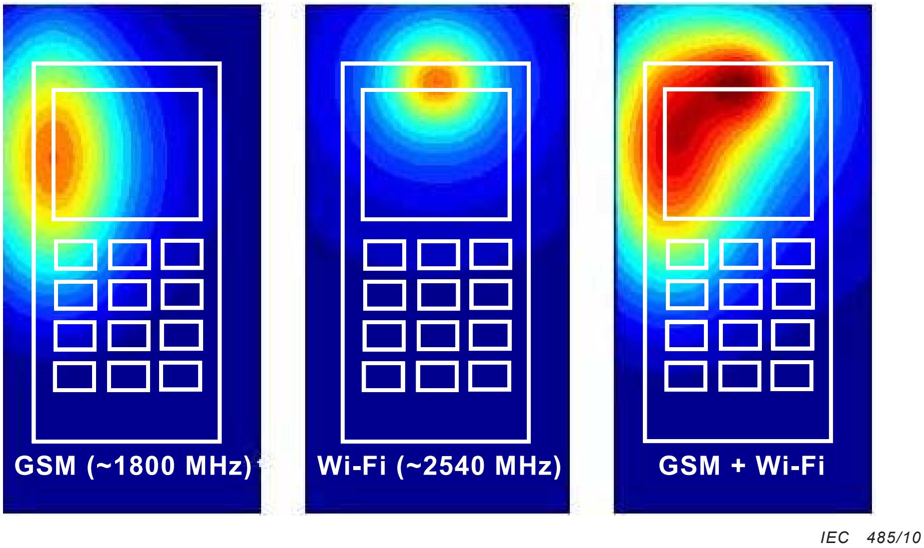

Figure C.2 – Qualitative description of the individual and combined *SAR* distributions for a mobile phone transmitting simultaneously GSM and Wi-Fi signals

9 In some cases, e.g. low-power Bluetooth transmitters, SAR distribution levels may fall below the measurement instrumentation sensitivity thresholds, typically indicating that the corresponding contribution to the overall SAR may be safely neglected. Further guidance may be provided in specific product standards, e.g. IEC 62209-2.

C.2.2 Combined power density for GSM and CDMA infrastructure antennas

This example addresses two co-located band-wide transmitters belonging to node-centric wireless communication devices.

Many antenna sites are shared by different operators. For instance, a communications tower hosting several operators is shown in Figure C.3. Suppose that an antenna site shared by two operators hosts two sets of transmit antennas, one transmitting GSM signals and the other transmitting CDMA signals. Since GSM and CDMA waveforms are uncorrelated, so are the corresponding EM fields and, therefore, the individual power density distributions can be summed as prescribed in Equation (5a). More specifically, suppose that *S* is measured over a set of points $R \equiv \{\mathbf{r}_n \mid n = 1, \cdots, N\}$ at the location(s) where the evaluation is performed, using suitable instrumentation that allows discriminating the GSM and CDMA waveforms, e.g., narrow-band and correlator receivers. Under these hypotheses, the individual power density data sets are:

GSM: $S_{\mathrm{GSM}}(R) \equiv \{S_{\mathrm{GSM}}(\mathbf{r}_n) \mid \mathbf{r}_n \in R\}$

CDMA: $S_{\mathrm{CDMA}}(R) \equiv \{S_{\mathrm{CDMA}}(\mathbf{r}_n) \mid \mathbf{r}_n \in R\}$

The combined power density distribution is then computed as the sum of the individual ones:

GSM+CDMA: $S_{\mathrm{GSM+CDMA}}(R) \equiv \{S_{\mathrm{GSM}}(\mathbf{r}_n) + S_{\mathrm{CDMA}}(\mathbf{r}_n) \mid \mathbf{r}_n \in R\}$

As mentioned in Subclause 6.4, the individual power density distributions should be suitably normalized, yielding exposure quotients, if frequency-dependent limits are applicable.

IEC 486/10

Figure C.3 – Communications tower shared by different network operators

C.3 Correlated sources

Smart antenna systems allow implementing space-time coding techniques to enhance wireless communication systems performance in terms of capacity, range, power efficiency, and reliability. Switched-beam and adaptive beamforming techniques are two approaches – of increasing technological complexity – frequently employed in smart antenna systems. Switched-beam antennas would typically feature a number of narrow beams that jointly fill the intended coverage sector, while adaptive beamformers employ digital signal processing techniques to realize suitably shaped radiation patterns to enhance the link margin while suppressing undesired interferers in real-time. In transmit mode, smart antenna systems feature antenna arrays whose feeding signals are properly weighted to introduce the amplitude profile and time delays that allow focusing the RF energy in the desired direction(s) while blinding interferers by suitably placing pattern null(s). For what concerns RF exposure, the main observation is that the physical antennas are formed by several elements (e.g., the antenna sketched in Figure C.4) that transmit the same signal albeit with different amplitudes and delays, which vary adaptively in real-time. At a measurement point, the relative strength and phase of the fields emitted by each element vary in time. Therefore, the evaluation approaches discussed in Subclause 6.4 can be applied, as illustrated in the following.

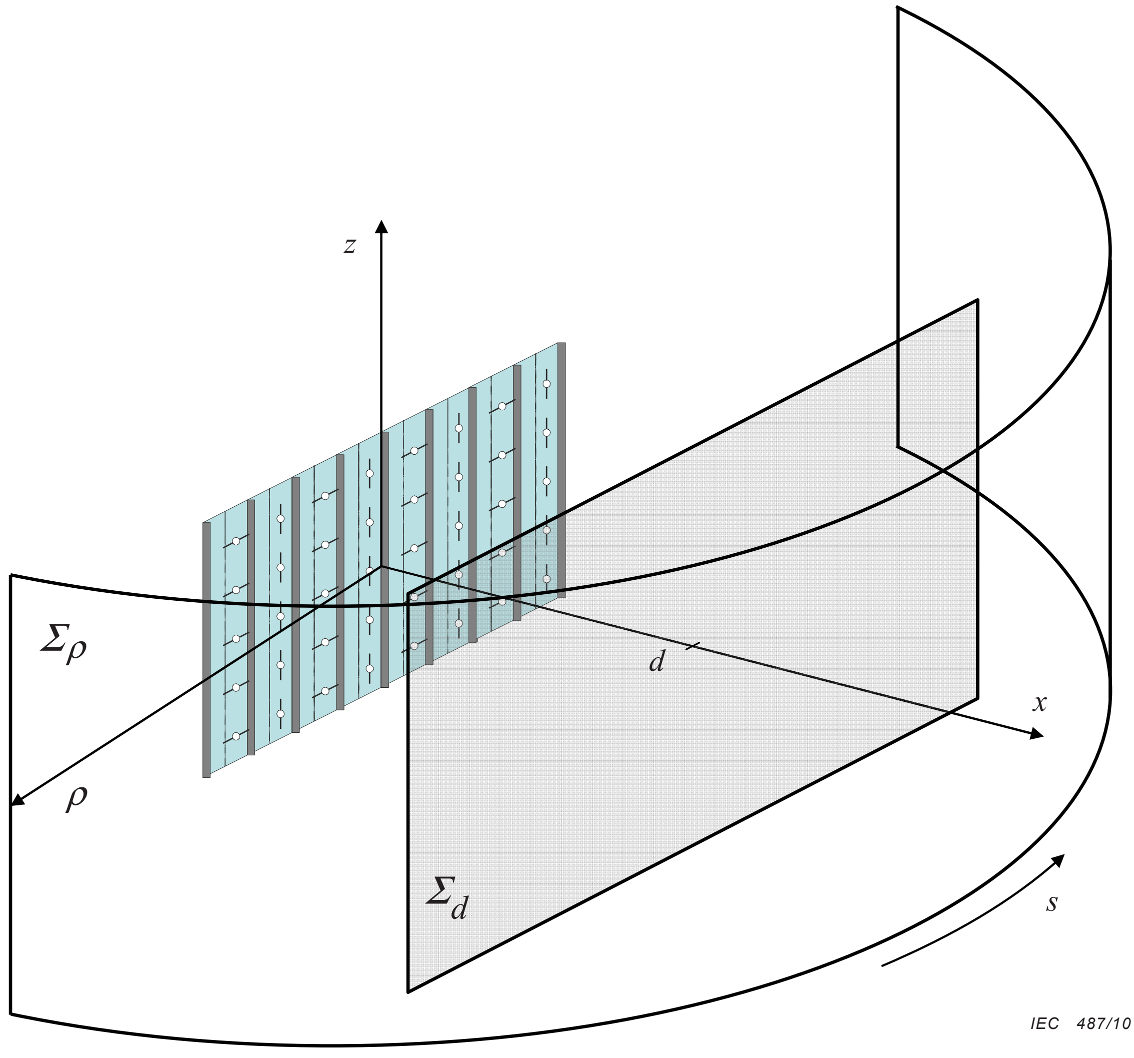

Figure C.4 – Smart antenna formed by 8 vertical 5-element ground-backed dipole arrays

The arrays exhibit alternate horizontal and vertical polarisation. The surfaces Σ_d (flat) and Σ_ρ (cylindrical) represent two possible exposure evaluation areas.

C.3.1 Exposure to smart antennas

Consider a two-element smart antenna system such as that in Figure 1. Each antenna element emits a replica of the same signal albeit with different magnitude and phase. The application of Equation (6) to yield a conservative estimate of exposure at a given set of evaluation points $R \equiv \{\mathbf{r}_n \mid n = 1, \cdots, N\}$ requires that the antenna elements are operated at the respective peak power levels and that the relative phase difference ($\Delta\phi_{12} = \phi_1 - \phi_2$) is varied so the maximum combined field magnitude is attained at each point:

$$S_{\max}(R) \equiv \left\{ \max_{\Delta\phi_{12} \in [0, 2\pi)} \left(\frac{1}{\eta_0} \left| \mathbf{e}_1(\mathbf{r}_n; \phi_1) + \mathbf{e}_2(\mathbf{r}_n; \phi_2) \right|_{rms}^2 \right) \mid \mathbf{r}_n \in R \right\} \quad \text{(C1)}$$

When the exposure evaluation is carried out using measurements, the above procedure could be implemented using scalar E-field probes by setting the transmitter to each antenna element to the maximum average power and performing a measurement for different values of the phase difference, e.g., every 10° (resulting in 36 measurements). It is readily seen that this procedure may be very time consuming, and would rapidly become unpractical as the number of antenna elements is increased, since a correspondingly growing number of relative phase differences ($\Delta\phi_{ij}$) between antenna elements would have to be sampled. Furthermore, such an experimental setup would require control of the smart antenna electronics, which might be possible in a suitable laboratory setting but difficult or impossible at an antenna site.

A more efficient approach would involve the use of *vector* sensors to measure magnitude *and* phase of the field components for each antenna element at every point $\mathbf{r}_n$, and carrying out the aforementioned relative phase sampling and the corresponding vector field summation computationally. As discussed earlier, vector sensors may not be readily available so this approach may not be always viable.

Electromagnetic simulations yielding magnitude and phase of the field emitted by each antenna element could also represent an efficient alternative. However, significant effort to develop and validate the antenna simulation model might still be required.

C.3.2 Application of the alternative approaches [6.5.2.2 or 6.5.2.3]

This example addresses several co-located band-wide transmitters embedded in a node-centric wireless communication device.

The smart antenna in Figure C.4, featuring eight vertical five-element dipole arrays with alternating polarisation, each backed by a ground-plane, is analysed in the following to determine the outcome of exposure evaluations carried out using the true vector sum [Equation (6)] or the alternative approaches described in Subclause 6.5.2. The antenna operates at 3,5 GHz, and the distance between array elements is one wavelength. Suppose measurements are performed across the cylindrical surface Σ_ρ at a distance ρ = 1 m from the antenna over a ±80° angular span from the broadside direction (x-axis), corresponding to 2,8 m along the circular abscissa s, and across a 1 m vertical extension along z. The results in Figure C.5 show the power density distribution for the true vector sum [Equation (6)] and those produced by summing the field magnitudes [Equation (10)] or the homonymous field-component magnitudes [Equation (12)].

The true vector sum distribution was compiled from a Monte-Carlo analysis involving the total field computation for 100 000 random realisations of the antenna elements phase profiles $\{\phi_1, \cdots, \phi_8\}$, while feeding all eight array elements at the respective maximum RF power settings, and taking the peak realised power density, i.e., the maximum power density produced at each evaluation point $\mathbf{r}_n \in \Sigma_\rho$ by any one of the random phase profiles.

Observe that the power density over the area Σ_ρ exhibits the same spatial distribution regardless of the evaluation approach, but the absolute levels are different. As expected, Equation (10) provides a larger overestimation than Equation (12), showing the benefit of using the latter whenever practical. In this particular example, the overestimation produced by Equation (12) is quite smaller, 3 % (0,13 dB) versus 107 % (3,2 dB) for the respective peak values over the evaluation area Σ_ρ , as shown in Figure C.6. In both cases, the overestimation is within about 3 dB, which may represent an acceptable trade-off against the faster measurement method requiring only a single scan per array element (8 total scans in the example) using scalar isotropic probes.

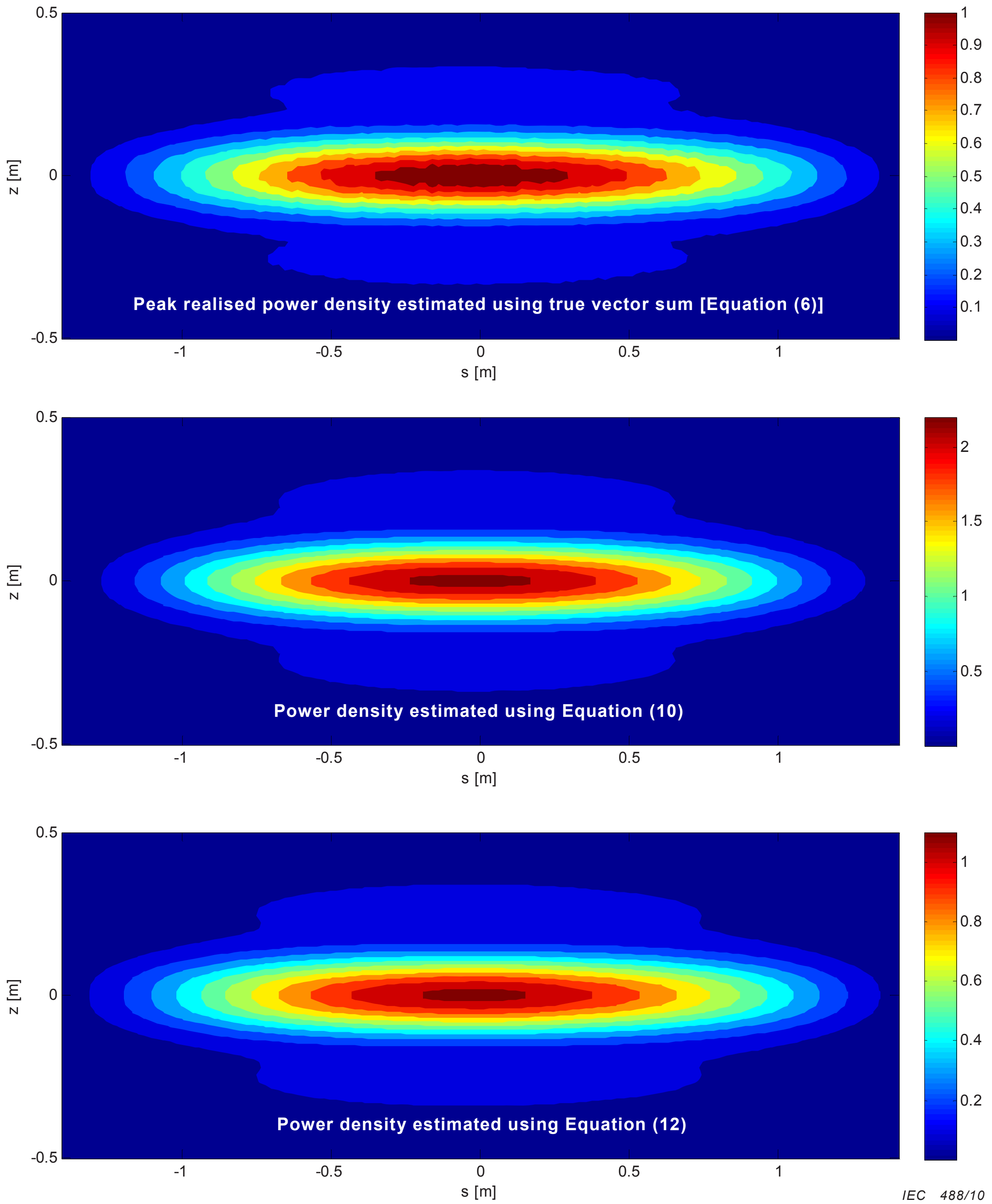

Figure C.5 – Power density distributions on the surface Σ_ρ (ρ = 1 m) derived via Equations (6), (10), and (12) for the 3,5 GHz smart antenna shown in Figure C.4

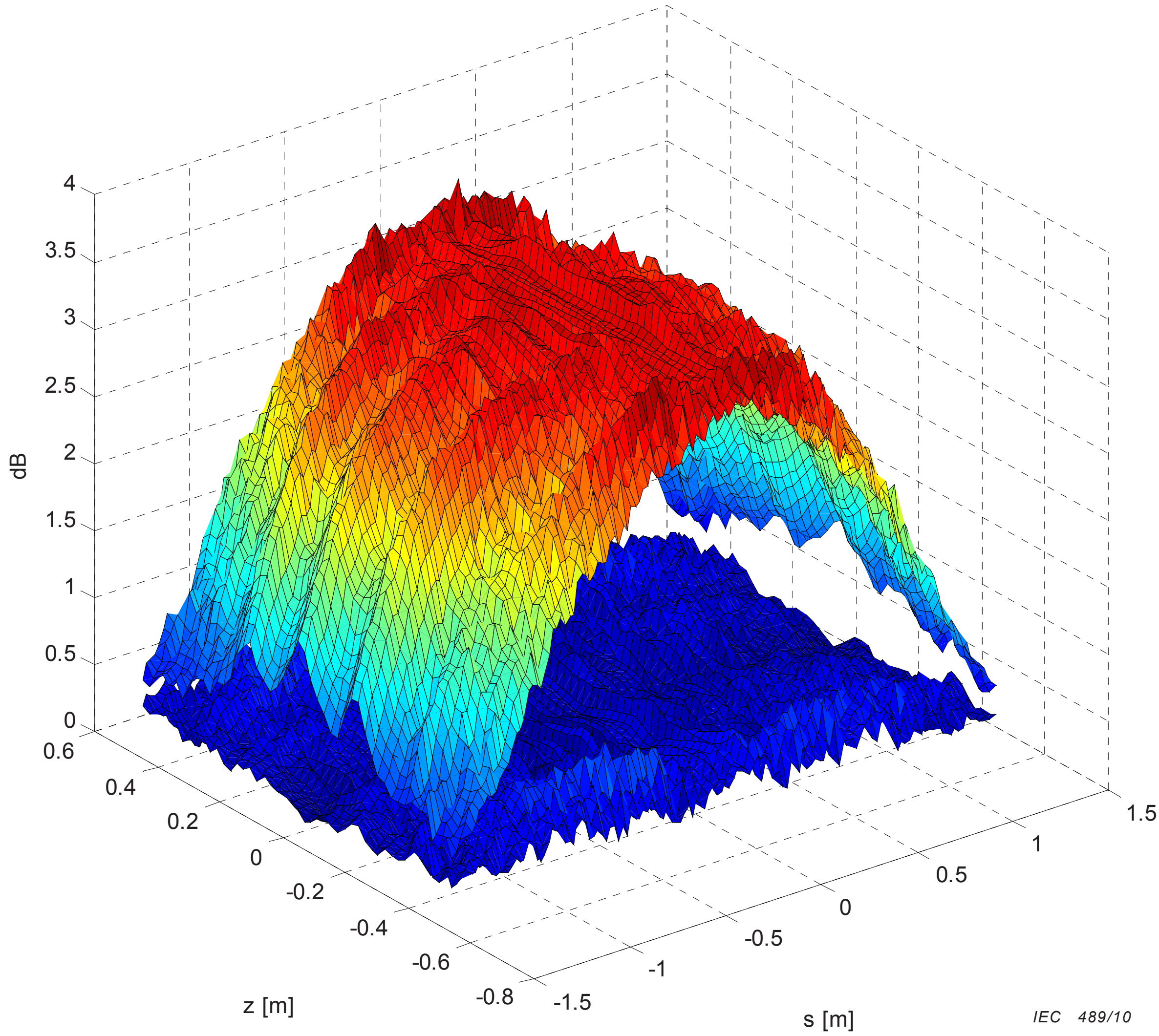

Figure C.6 – Overestimations produced by Equations (10) and (12) over the exposure evaluation area Σ_ρ (ρ = 1 m) for the 3,5 GHz smart antenna shown in Figure C.4

In this example, the maximum power setting was employed for each element of the smart antenna. Such an approach leads to very conservative exposure evaluations since it neglects one of the fundamental characteristics of modern wireless communications systems, i.e. the fact that their capacity is interference-limited. Thus, emitted power levels from smart antennas are adjusted in real-time to assure just enough signal quality at the intended receive mobile station while delivering the least amount of interference to the remaining ones. It should be expected that statistical rationales may be adopted in applicable standards to justify the use of lower antenna element power settings, while still yielding a conservative exposure evaluation.

Bibliography

IEC 62209-2:2010, *Human exposure to radio frequency fields from handheld and body-mounted wireless communication devices – Human models, instrumentation, and procedures – Part 2: Procedure to determine the specific absorption rate (SAR) for wireless communication devices used in close proximity to the body (frequency range of 30 MHz to 6 GHz)*[10)]

IEC 62232, *Determination of RF field strength and SAR in the vicinity of radio communication base stations for the purpose of evaluating human exposure*[11)]

IEEE Std C95.3:2002, *Recommended Practice for Measurements and Computations of Radio Frequency Electromagnetic Fields with respect to human exposure to such fields, 100 kHz – 300 GHz*

---

10) To be published.

11) To be published.

This page deliberately left blank

British Standards Institution (BSI)

BSI is the independent national body responsible for preparing British Standards and other standards-related publications, information and services.
It presents the UK view on standards in Europe and at the international level.

It is incorporated by Royal Charter.

Revisions

British Standards are updated by amendment or revision. Users of British Standards should make sure that they possess the latest amendments or editions.

It is the constant aim of BSI to improve the quality of our products and services. We would be grateful if anyone finding an inaccuracy or ambiguity while using this British Standard would inform the Secretary of the technical committee responsible, the identity of which can be found on the inside front cover.

Tel: +44 (0)20 8996 9001 Fax: +44 (0)20 8996 7001

BSI offers Members an individual updating service called PLUS which ensures that subscribers automatically receive the latest editions of standards.

Tel: +44 (0)20 8996 7669 Fax: +44 (0)20 8996 7001
Email: plus@bsigroup.com

Buying standards

You may buy PDF and hard copy versions of standards directly using a credit card from the BSI Shop on the website **www.bsigroup.com/shop.** In addition all orders for BSI, international and foreign standards publications can be addressed to BSI Customer Services.

Tel: +44 (0)20 8996 9001 Fax: +44 (0)20 8996 7001
Email: orders@bsigroup.com

In response to orders for international standards, it is BSI policy to supply the BSI implementation of those that have been published as British Standards, unless otherwise requested.

Information on standards

BSI provides a wide range of information on national, European and international standards through its Knowledge Centre.

Tel: +44 (0)20 8996 7004 Fax: +44 (0)20 8996 7005
Email: knowledgecentre@bsigroup.com

Various BSI electronic information services are also available which give details on all its products and services.

Tel: +44 (0)20 8996 7111 Fax: +44 (0)20 8996 7048
Email: info@bsigroup.com

BSI Subscribing Members are kept up to date with standards developments and receive substantial discounts on the purchase price of standards. For details of these and other benefits contact Membership Administration.

Tel: +44 (0)20 8996 7002 Fax: +44 (0)20 8996 7001
Email: membership@bsigroup.com

Information regarding online access to British Standards via British Standards Online can be found at **www.bsigroup.com/BSOL**

Further information about BSI is available on the BSI website at **www.bsigroup.com/standards**

Copyright

Tel: +44 (0)20 8996 7070
Email: copyright@bsigroup.com

BSI Group Headquarters

389 Chiswick High Road London W4 4AL UK

Tel +44 (0)20 8996 9001
Fax +44 (0)20 8996 7001
www.bsigroup.com/standards

raising standards worldwide™